Specific combinations of Ca^{2+} channel inhibitors reduce excessive Ca^{2+} influx as a consequence of oxidative stress and increase neuronal and glial cell viability *in vitro*

Ryan L. O'Hare Doig,[1,2,3] Carole A. Bartlett,[1,2] Nicole M. Smith, [1,2, 4] Stuart I. Hodgetts,[1,3] Sarah A. Dunlop,[1,2] Livia Hool,[3,5] and Melinda Fitzgerald[1,2]

[1]Experimental and Regenerative Neurosciences, [2]School of Animal Biology, [3]School of Anatomy, Physiology and Human Biology, [4]School of Chemistry and Biochemistry, The University of Western Australia, Crawley, Western Australia, Australia, [5]Victor Chang Cardiac Research Institute, Sydney, New South Wales, Australia

Corresponding Author: Melinda Fitzgerald - lindy.fitzgerald@uwa.edu.au

Experimental and Regenerative Neurosciences, School of Animal Biology, The University of Western Australia, Crawley, 6009 Western Australia, Australia

Phone: 61 8 6488 2353

Highlights *(note, these are limited to 85 characters each)*

The effects of combinations of Ca^{2+} channel inhibitors on H_2O_2 stressed cells were assessed *in vitro.*

Most combinations of inhibitors with oxATP decreased Ca^{2+} influx and increased cell viability.

However, reductions in intracellular Ca^{2+} concentration were not always linked to cell viability.

Combinations of inhibitors preserved some cell subpopulations, particularly NG2+/olig2- glia.

The data increase understanding of the efficacy of Ca^{2+} channel inhibitor combinations *in vivo*

Abstract

Combinations of Ca^{2+} channel inhibitors have been proposed as an effective means to prevent excess Ca^{2+} flux and death of neurons and glia following neurotrauma *in vivo*. However, it is not yet known if beneficial outcomes such as improved viability have been due to direct effects on intracellular Ca^{2+} concentrations. Here, the effects of combinations of Lomerizine (Lom), YM872, memantine and/or oxATP to block voltage gated Ca^{2+} channels, Ca^{2+} permeable AMPA receptors, NMDA receptors and purinergic $P2X_7$ receptors ($P2X_7R$) respectively, on Ca^{2+} concentration and viability of primary mixed cortical cultures exposed to hydrogen peroxide (H_2O_2) insult, were assessed. The contribution of Ryanodine sensitive intracellular stores to intracellular Ca^{2+} concentration was also assessed. Live cell calcium imaging revealed that a 30 minute H_2O_2 insult induced a slow increase in intracellular Ca^{2+}, in part from intracellular sources, associated with loss of cell viability by 6 hours. Most combinations of inhibitors that included oxATP significantly decreased Ca^{2+} influx and increased cell viability when administered simultaneously with H_2O_2. However, reductions in intracellular Ca^{2+} concentration were not always linked to improved cell viability. Examination of the density of specific cell subpopulations demonstrated that most combinations of inhibitors that included oxATP preserved NG2+ non-oligodendroglial cells, but preservation of astrocytes and neurons required additional inhibitors. $Olig2^+$ oligodendroglia and $ED\text{-}1^+$ activated microglia/macrophages were not preserved by any of the inhibitor combinations. These data indicate that following H_2O_2 insult, limiting intracellular Ca^{2+} entry *via* $P2X_7R$ is generally associated with increased cell viability. Protection of NG2+ non-oligodendroglial cells by Ca^{2+} channel inhibitor combinations may contribute to observed beneficial outcomes *in vivo*.

Keywords

Ca^{2+} channel inhibitors; intracellular Ca^{2+} concentration; oligodendroglia; NG2-glia; cell viability

Abbreviations

AMPA, α-amino-3-hydroxy-5-methyl-4-isoxazolepropionic acid; AMPARs, α-amino-3-hydroxy-5-methyl-4-isoxazolepropionic acid receptors; ANOVA, analysis of variance; ATP, adenosine 5'-triphosphate; Ca^{2+}, calcium; CNS, central nervous system; DMSO, dimethyl sulfoxide; FOV, field of view; HBSS, Hanks balanced salt solution; h, hours; Lom, Lomerizine; MC, mixed cortical; Memantine (Mem), 3,5-dimethyl-1-adamantanamine; min, minutes; NB, Neurobasal® medium; NMDA, *N*-methyl-D-aspartate; NMDARs, *N*-methyl-D-aspartate receptors; oxATP, adenosine 5'-triphosphate periodate oxidized sodium salt; PFA, paraformaldehyde; PBS, phosphate buffered saline; PVG, Piebald Viral Glaxo; $P2X_7R$, $P2X_7$ receptors; ROI, region of interest; SCI, spinal cord injury; SEM, standard error of the mean; VGCCs, voltage-gated Ca^{2+} channels; YM872, 2,3-dioxo-7-(1*H*-imidazol-1-yl)6-nitro-1,2,3,4-tetrahydro-1-quinoxalinyl]acetic acid monohydrate;

Introduction

In the CNS, calcium (Ca^{2+}) plays a vital role in important physiological processes such as cell differentiation, growth and survival (Komuro and Rakic, 1996; Gomez and Spitzer, 2000; Spitzer et al., 2000). Changes in cytosolic Ca^{2+} stimulate multiple Ca^{2+}-dependent pathways, normally designed to maintain cell structure and function. These include, but are not limited to, calpain activation (Lipton, 1999), lipid peroxidation (Braughler and Hall, 1992), nitric oxide synthesis (Bolanos et al., 1997) and mitochondrial free radical production (Camello-Almaraz et al., 2006). However, Ca^{2+} also plays a salient role in cell death, with excessive intracellular Ca^{2+} accumulation leading to over-activation of Ca^{2+} dependent pathways that are the final common mechanism for damage and/or death of a variety of CNS cell types (Tekkok and Goldberg, 2001; Prilloff et al., 2007). Following neurotrauma, neurons and glia close to the site of insult are vulnerable to secondary degeneration and may undergo delayed

death *via* a multitude of these Ca^{2+} dependent cellular and molecular cascades. Downstream mechanisms of damage include glutamate excitotoxicity (Doble, 1999; Hausmann, 2003; Matute et al., 2006), inflammation (Hausmann, 2003), Wallerian degeneration (Kerschensteiner et al., 2005; Weishaupt et al., 2010), glial scarring (Fawcett and Asher, 1999), dysmyelination (Totoiu and Keirstead, 2005; Payne et al., 2011), and apoptosis (Liu et al., 1997).

Ca^{2+} is known to enter neurons and glia through a range of channels and receptors, including but not limited to: voltage-gated Ca^{2+} channels (VGCCs) (Agrawal et al., 2000); purinergic $P2X_7$ receptors (Matute et al., 2007); glutamate-gated, GluR2 subunit lacking, Ca^{2+} permeable ionotropic α-amino-3-hydroxy-5-methyl-4-isoxazolepropionic acid receptors (AMPARs) (Hollmann et al., 1991); and *N*-methyl-D-aspartate receptors (NMDARs) (Matute, 2006). Increased glutamate is a common consequence following injury to the CNS (Doble, 1999) and can lead to over-activation of NMDA and AMPA receptors on neurons and glia, specifically oligodendrocytes, rendering these cells susceptible to increased Ca^{2+} influx and depolarisation (Matute et al., 1997; Doble, 1999). ATP also typically increases in response to injury (Neary et al., 2005), which can directly injure vulnerable cells, as well as trigger ATP-gated Ca^{2+} influx (Matute et al., 2007). Reactive species such as cell permeant H_2O_2 are generated as a consequence of injury both *in vivo* (Cornelius et al., 2013; O'Hare Doig et al., 2014a) and *in vitro* (Mandavilli et al., 2005; Ma et al., 2012), and also lead to increased influx through Ca^{2+} channels (Muralidharan et al., 2016). As such, over-activation of Ca^{2+} channels and receptors results in an appreciable influx of Ca^{2+} into cells. As a consequence of both Ca^{2+} and reactive species entry, mitochondria swell, oxidative metabolism is compromised, and cytochrome *c* is released into the cytoplasm, associated with oxidative damage to DNA, lipids and proteins, and neuronal and glial cell death (Gandhi et al., 2009; Huang et al., 2009; Kowaltowski et al., 2009a).

Given the consequences of excessive Ca^{2+} entry into neurons and glia following injury, the administration of Ca^{2+} channel inhibitors has been assessed as a therapeutic strategy for treatment of CNS damage *in vivo*. In rodent models of ischemia, application of nimodipine, an L-Type VGCC inhibitor, resulted in significant functional recovery (Ouardouz et al., 2003) and attenuated mitochondrial injury and apoptosis (Tanaka et al., 2004). However, nimodipine has also been found to cause hypotension and further ischemic injury to the spinal cord (Fehlings et al., 1989). Lomerizine (Lom), a dual L- and T-type VGCC inhibitor which

is currently in clinical use for the treatment of migraines, has been shown to act more specifically on the CNS with adverse systemic side effects avoided (Hara et al., 1999). We have demonstrated reduced retinal ganglion cell death and microglia/macrophage infiltration, preservation of myelin compaction and limited functional improvements following treatment of partial CNS injury with lomerizine (Fitzgerald et al., 2009), but clinical trials of lomerizine for treatment of neurotrauma are lacking.

A relatively limited number of $P2X_7R$ antagonists have been developed (Baraldi et al., 2000; Baraldi et al., 2002; Baraldi et al., 2003). One of the more effective of these is adenosine 5'-triphosphate periodate oxidized sodium salt (oxATP), an irreversible, non-competitive antagonist of $P2X_1$, $P2X_2$ and $P2X_7$ receptors, which has been shown to protect against secondary injury, and improve functional outcomes in rats following acute impact spinal cord injury (SCI) (Wang et al., 2004). NBQX, an AMPAR antagonist, has been shown to have neuroprotective effects following cerebral ischemia (Gill, 1994; Graham et al., 1996) and reduce excitotoxic insult in white matter following injury (Follett et al., 2000). However, NBQX has poor water solubility, and renal toxicity has limited use of this drug in the clinic (Xue et al., 1994). More recently, a highly selective novel competitive AMPA receptor antagonist [2,3-dioxo-7-(1*H*-imidazol-1-yl)6-nitro-1,2,3,4-tetrahydro-1-quinoxalinyl] acetic acid monohydrate (YM872 or "INQ"), with high solubility, was developed. YM872 has been assessed in a number of clinical trials of neuroprotection (Takahashi et al., 1998), however it was abandoned in phase-III human clinical trials for stroke in 2010, after failing an interim futility analysis (Klein and Engelhard, 2010). 3,5-dimethyl-1-adamantanamine (memantine or "Mem") is a non-competitive NMDAR antagonist, shown to provide neuroprotection with minimal side effects in animal models of ischemia (Block and Schwarz, 1996; Ehrlich et al., 1999). Memantine therapy has shown beneficial effects after brain injury, including alleviation of neurobehavioral deficits (Huang et al., 2015).

Whilst promising results have been demonstrated in pre-clinical studies, the translation of these therapeutic agents to the clinic has been limited and outcomes have been disappointing, highlighting the clear need for a new approach. Given the multiple routes of Ca^{2+} entry associated with the detrimental aspects of neurotrauma, it is becoming increasingly recognized that a combinatorial treatment strategy may be required (Tuszynski, 2005; Stack et al., 2006). We recently tested this hypothesis *in vivo*, assessing the efficacy of various combinations of three Ca^{2+} channel inhibitors at reducing secondary degeneration assessed 3 months following partial optic nerve transection in Piebald Viral Glaxo (PVG) rats (Savigni

et al., 2013). We used Lom to inhibit L- and T-type VGCCs, oxATP to inhibit $P2X_7Rs$, and/or YM872, to inhibit Ca^{2+} permeable AMPARs. Each of the treatment combinations involving lomerizine significantly increased the proportion of axons with normal compact myelin, implying a role for excess Ca^{2+} entry *via* VGCCs in myelin decompaction. In areas of nerve vulnerable to secondary degeneration, there is a significant increase in node of Ranvier length, associated with loss of visual function (Szymanski et al., 2013). Only administration of the three Ca^{2+} channel inhibitors in combination (Lom + oxATP + YM872) resulted in maintenance of normal node of Ranvier length(s), and preservation of function, with the remaining combinations proving less effective (Savigni et al., 2013).

However, an association between intracellular Ca^{2+} concentration and the viability of neurons and glia following treatment with combinations of Ca^{2+} channel inhibitors has not yet been established. Therefore here, the effects of combinations of the inhibitors (Lom, OxATP, YM872 and/or Mem) on excess Ca^{2+} influx and associated cell death of multiple cell types were determined, using a high throughput, *in vitro* model of oxidative injury in primary mixed cortical cultures (Whittemore et al., 1994). Note that the phrase "Ca^{2+} channel inhibitors" is used throughout, with the understanding that Ca^{2+} permeable AMPARs, $P2X_7Rs$ and NMDARs are also permeable to other ions that may be playing a role. Hydrogen peroxide (H_2O_2) was chosen as the reactive species stressor given its relative stability and established role in inducing oxidative damage in neurons and glia (Haskew-Layton et al., 2010).

Materials and Methods

Animals

PVG rat pups (postnatal days 0-3) were obtained from the Animal Resource Centre (Murdoch, Western Australia). All procedures were approved by The University of Western Australia Animal Ethics Committee (Ethics Approval Number RA3/100/673) and conformed to the National Health and Medical Research Council (NHMRC) of Australia Code of Practice for use of Animals for Scientific Purposes. All efforts were made to minimise animal suffering and to reduce the number of animals used. Rat pups were euthanized with intraperitoneal injection of Lethabarb© (Pentobarbital sodium 850mg/kg, Virbac). For each

cell culture preparation, cortices from two to six animals were pooled together, depending upon cell numbers required. 85 animals were used in the experiments of the study.

Tissue dissection

Following euthanasia, the skin overlying the skull was removed, and the skull was peeled away. Deep cuts were made at the margin of the cortex and superior colliculi caudally (both sides) and again at the border of the olfactory lobes, and cortex rostrally. The middle section of the brain with cortices intact was removed from the skull, and transferred to a sterile petri dish containing cold (~4˚C) Neurobasal®-A medium (NB-A, Life Technologies). The cortex was then peeled away from underlying midbrain structures and the meninges were teased off. The 'naked' cortex was then transferred to a second sterile petri dish containing cold NB-A. Once all tissue was collected, a scalpel blade was used to chop the cortices into small pieces, which were transferred using a transfer pipette to a 50mL falcon tube containing 10mL NB-A.

Cell culture

Mixed cortical (MC) cells were prepared as described in (Whittemore et al., 1994). In brief: following an initial 3 minute (min), 200g centrifugation, tissue was enzymatically digested in 10mL Phosphate Buffered Saline (PBS; Invitrogen) solution containing 165U papain (Worthington), 3000U of DNase 1 from bovine pancreas (dissolved in Earls Balanced Salt Solution; both from Sigma-Aldrich), 1.65µM cysteine (Sigma-Aldrich) and 50µM NaOH for 5 minutes (min), at 37˚C. Enzyme treated tissue pieces were centrifuged for 22 min at 200g, enzyme solution was removed and tissue was dissociated in 10mL of NB2 media, consisting of: Neurobasal®-A medium (NB-A), containing 500µM glutamine (Life Technologies), 2% B27 (Life Technologies), 100U/mL penicillin (Invitrogen) and 100µg/mL streptomycin; (Invitrogen). All multi-well plates and coverslips were pre-coated with poly-L-lysine (10µg/mL) in UltraPure™ distilled water, for one hour (h) at room temperature, followed by washing 3x with PBS prior to cell seeding. MC cells were seeded at $1.5x10^5$ cells/cm^2 in NB2: into 12 well plates containing 15mm coverslips (for calcium imaging); or 24 well plates (for live/dead viability assay). Following seeding, cells were allowed to incubate for 24 h after which NB2 media was replaced with fresh media containing 57% NB2 and 43% NB1 media (NB2/NB1 growth media). NB1 media is NB2 media supplemented with 4.2% fetal calf serum (Life Technologies), 1% (v/v) horse serum (Life Technologies), 26.7µM L-

glutamic acid monosodium salt hydrate (Sigma-Aldrich), and 22.2µM 2-mercapathoethanol (Life Technologies). NB2/NB1 media was replaced every 48-72 h.

Treatments

Effects of combinations of Ca^{2+} channel inhibitors, Lom (LKT Labs), OxATP (Sigma), YM872 (LKT Labs), and/or Mem (Sigma) were assessed. Choices of treatment concentrations were based on previously published studies using these agents individually. Lom was dissolved in dimethyl sulfoxide (DMSO) before being added to medium at a final concentration of 1µM (Tamaki et al., 2003): final concentration of DMSO was less than 1% v/v. OxATP (1mM; (Matute et al., 2007)), YM872 (240µM; (Savigni et al., 2013)) and Mem (60µM, (McAllister et al., 2008)) were dissolved in medium. Ca^{2+} channel inhibitors were administered to cultures such that all possible combinations of single and multiple inhibitors were assessed.

Analysis of inhibitor and H_2O_2 stability

Stability of the inhibitors in the presence and absence of H_2O_2 were assessed by reverse phase High Performance Liquid Chromatography (HPLC), on a Waters 2695 HPLC with a Waters 2489 UV/vis detector with elution through a C18 analytical column (150 x 4.60 mm, 5 µm, 25°C). For all inhibitors, the ratio of inhibitor:H_2O_2 concentration equated to those used in cell analysis experiments, described below. For OxATP, two samples were prepared by dissolving OxATP in water in the absence and presence of H_2O_2 (OxATP:H_2O_2, 1:0.4). A mobile phase of Acetonitrile (A):0.1M Phosphate buffer pH 7 (B) was used with gradient elution and varying flow rates as follows: 0 mins, 100% B at 0.85ml/min; 4 mins, 95% B at 0.8 ml/min; 8 mins, 75% B at 1mL/min; 12 mins, 70% B at 1 ml/min. Injection volume was 10µL, detection wavelength was 254nm with retention times of 5.4 min (OxATP) and 5.2 min (OxATP + H_2O_2). Total run time was 12 mins.

For Lomerizine and YM872 the mobile phase consisted of Water with 0.5% Trifluoroacetic acid:Acetonitrile (31:69 v/v) with isocratic elution at 0.5ml/min. Total run time was 15 mins, detection wavelength was 210nm and sample injection volume was 1µL. Lomerizine was dissolved in methanol in the absence and presence of H_2O_2 (Lom:H_2O_2, 1:400) with retention times of 4.7 mins. However, an additional peak at 3.3 min was evident in the presence of H_2O_2 indicating possible degradation of lomerizine. YM872 was dissolved in water in the absence and presence of H_2O_2 (YM872:H_2O_2, 1:1.65) with retention times of 2.9 mins.

Stability of H_2O_2 in the presence and absence of the compounds was measured by fluorescence detection of H_2O_2 using the hemin-catalyzed oxidation of p-hydroxyphenylacetic acid to yield the fluorescent dimer. Briefly, p-hydroxyphenylacetic acid (80μM) and hemin (8μM) were dissolved in ammonia buffer, pH 10. This solution was then used to prepare samples of H_2O_2 (400μM) in the absence and presence of: YM872, OxATP, Lomerizine (see compound:H_2O_2 ratios detailed above) and Memantine (Memantine:H_2O_2, 1:6.7). Fluorescence was measured in triplicate on a Varian Cary Eclipse instrument with excitation at 320nm and emission at 410nm in a 1mL cuvette with a 10mm path length. Average fluorescence intensity was 40 ± 0.5 in the absence and presence of each of the compounds.

Cell analysis

The following experiments were undertaken following 10 days of culture in NB2/NB1growth media at 37˚C (95% air/5% CO_2 v/v). Control cultures were incubated in identical fashion but without H_2O_2, and/ or without the addition of Ca^{2+} channel inhibitors or other modulators as detailed below.

Live Ca^{2+} imaging: Ca^{2+} imaging was performed on MC cells attached to glass coverslips at room temperature, using the ratiometric Ca^{2+} sensitive dye Fura-2AM (Invitrogen). All solutions were prepared immediately prior to imaging. Cells were loaded with 4μM Fura-2AM in NB-A (+10mM HEPES, without phenol red; Life Technologies) at room temperature, for 30 min, then gently washed with Hanks Balanced Salt Solution (HBSS; Life Technologies). Coverslips were then transferred to an RC-26G chamber system (Warner Instruments) containing 1mL NB-A (+10mM HEPES). Images were captured every 15 seconds for 2 min in order to measure basal Ca^{2+} levels. A pre-prepared solution containing a final H_2O_2 concentration of 400μM ± Ca^{2+} channel inhibitors (at concentrations described above), and/ or the ryanodine receptor agonist ryanodine (20μM, 40μM, or 60μM; Sigma-Aldrich) or the Zn chelator N,N,N',N'-Tetrakis(2-pyridylmethyl)ethylenediamine (TPEN, 1 or 10μM; Sigma-Aldrich) was then applied to the chamber at the beginning of a 30 min acquisition. The choice of H_2O_2 concentration was based upon previous studies and our own pilot experiments that indicated 400μM provides a sustained and consistent increase in intracellular Ca^{2+} without biphasic effects or oscillations (Herson et al., 1999). In initial experiments, individual intracellular Ca^{2+} concentrations were determined. MC cells were incubated with Fura-2 AM as above and imaged for 10min following addition of 10μM

ionomycin (Molecular Probes) in HBSS (+3mM Ca^{2+}, Mg^{2+}) to determine R_{max} values. MC cells were then washed gently with HBSS (Ca^{2+} free) and imaged for another 10 min following addition of 10µM BAPTA AM (Molecular Probes). The mean intracellular Ca^{2+} concentration at baseline (no H_2O_2 present) was ~73nM.

Cells were visualized using an Olympus BX51WI upright microscope equipped with an XM10 monochrome CCS camera (Olympus). Imaging was performed at x60 magnification, capturing a field of view of 147.2µm x 100.4µm, with an exposure time of 20ms and 2x2 pixel binning. Regions of interest (ROIs) per field of view (FOV) were defined for each individual cell within the FOV, and were used to determine F340/F380 ratios using Olympus Xcellence RT software. One FOV per coverslip was assessed, consistent for all coverslips.

Cell viability: MC cells were incubated in H_2O_2 ± Ca^{2+} channel inhibitors and/or Ethylene glycol-bis(2-aminoethylether)-*N,N,N',N'*-tetraacetic acid (EGTA; 10µM, 0.1mM or 1mM; Sigma-Aldrich) for 30 min, 6 or 24 h. Immediately following the incubation, cells were gently rinsed with HBSS, and incubated with 1µM Calcein-AM (Invitrogen) and 2µM Ethidium homodimer (Ethd-1; Invitrogen) for 30 min. Cultures were then imaged at x40 magnification using an Olympus IX51 inverted fluorescence microscope. FOV were randomly assigned and consistent for all culture wells. Viability was quantified by counting all viable and dead cells in 2 FOV per well (450µm x 350µm), with three wells per condition. Data were expressed as the percentage of viable cells ± S.E.M.

Densities of individual cell populations: MC cells were incubated in H_2O_2 ± Ca^{2+} channel inhibitors for 30 min, 6 or 24 h. Following incubation, cell cultures were washed 3x with PBS, then fixed with 2% v/v paraformaldehyde (PFA; 0.1M phosphate buffer; pH 7.2) for 10 min, followed by a further 20 min with 4% v/v PFA (0.1M phosphate buffer; pH 7.2). Cells were then washed a further 3x with PBS and immunohistochemical analyses conducted according to established procedures (Fitzgerald et al., 2010a), using primary antibodies to identify specific cell types: neurons, β-III tubulin (1:1000; Covance); astrocytes, glial fibrillary acidic protein (GFAP; 1:500; Sigma-Aldrich); NG2+ non-oligodendroglial cells, NG2+ (1:500; Abcam) / Olig2- (1:500, R and D Systems); oligodendroglia, Olig2; activated microglia/ macrophages (ED1; 1:500; Abcam) and Hoechst nuclear stain (1:2000; Invitrogen). Secondary antibodies were species specific AlexaFluor® 488 and 555 (1:400; Invitrogen). Cultures were imaged at x40 magnification using an Olympus IX51 inverted fluorescence microscope. Quantification of densities of individual cell populations was

conducted by counting all immunopositive cells in 4 FOV per well (450µm x 350µm), with 2 wells/treatment group. FOV were randomly assigned and consistent for all culture wells. Mean number of immunopositive cells were expressed per mm^2.

Statistical analyses

All statistical analyses were performed using SPSS® Version 20 (IBM©) analysis software. For analysis of live cell calcium imaging, all data were derived from 3-5 independent experiments, each experiment using cells prepared from separate groups of rat pups. Variability between experiments was examined and we did not find outliers from specific experiments. Because of the large number of inhibitor combinations being compared it was not feasible to conduct all assessments within each single experiment. Therefore, in accordance with best practice in the published literature (Zhang et al., 2005), data from the experiments were combined for the final statistical analyses. A minimum of 14 and frequently as many as 40 cells in total were assessed for each treatment condition. The baseline F340/F380 ratios were averaged and at each time point, F340/F380 ratios were divided by the mean baseline (F340/F380 ratio before addition of H_2O_2 +/- inhibitors) to give a ΔF-Ratio. As experiments were conducted on mixed cultures it was not appropriate to convert ΔF-Ratios to Ca^{2+} concentrations, due to established variabilities between Ca^{2+} concentrations in neurons and glia (Suadicani et al., 2010) and altered responses to stressors (van den Pol et al., 1992). ΔF-Ratios were compared using two-way repeated measures analysis of variance (ANOVA), with Games-Howell post-hoc tests ($\alpha = 0.05$) to compare $H_2O_2 \pm Ca^{2+}$ channel inhibitors to H_2O_2 treated cultures, at each time point assessed during the 30 min incubation period. Analyses of cellular viability were conducted using a two-way ANOVA ($\alpha = 0.05$), with Games-Howell post-hoc tests to compare $H_2O_2 \pm Ca^{2+}$ channel inhibitors to H_2O_2 control at each time point. Analyses of densities of individual cell types were conducted using a two-way ANOVA ($\alpha = 0.05$), with Dunnett's post-hoc tests to compare $H_2O_2 \pm Ca^{2+}$ channel inhibitors to H_2O_2 control at each time point. All data were expressed as means ± standard error of the mean (S.E.M.); F and degrees of freedom (df) are reported for each ANOVA conducted and subsequent p values refer to *post hoc* test outcomes.

Results

Differential reduction in intracellular Ca^{2+} with various Ca^{2+} channel inhibitor combinations

H_2O_2 insult resulted in gradual increases in mean ΔF-Ratio (indicative of changes in intracellular Ca^{2+} concentration) in MC cells over a 30 min incubation period, relative to control (Fig. 1B), with a significant increase demonstrated at 30 min ($df = 1$, $F = 15.67$, $p \leq 0.05$; representative images Fig. 1A). The intracellular Ca^{2+} concentration of MC cells not exposed to H_2O_2 did not change ($p > 0.05$, Fig. 1A, B). Increases in intracellular Ca^{2+} concentration can occur *via* influx across the cell membrane (extracellular source) or release from intracellular Ca^{2+} stores. The contribution of ryanodine receptor dependent release of Ca^{2+} from the endoplasmic reticulum was assessed by challenging the cultures with increasing concentrations of the antagonist ryanodine simultaneously with H_2O_2 insult. 40μM ryanodine was required to reduce the ΔF-Ratio at 30 min relative to H_2O_2 control ($df = 4$, $F = 32.27$, $p \leq 0.05$, Fig. 1B). However, the ΔF-Ratio in the presence of 40μM ryanodine remained higher than in controls without H_2O_2 at this time ($p \leq 0.05$, Fig. 1B), indicating additional sources of intracellular Ca^{2+}. Additional control experiments were conducted to assess the effect of ryanodine alone as well as the potential contribution of Zn to the Fura-2 signal, given that under some conditions Fura-2 can detect free Zn (Grynkiewicz et al., 1985). Addition of Ryanodine alone at the tested concentrations did not stimulate Ca^{2+} release above control levels at 30 min ($df = 4$, $F = 13.83$, $p > 0.05$, Fig. 1B). Addition of the Zn chelator TPEN to cultures simultaneously with H_2O_2 insult also did not significantly reduce the ΔF-Ratio at 30 min, relative to H_2O_2 alone ($p > 0.05$, Fig. 1C), indeed there was a non-significant trend to an increase with the chelator, indicating that the ΔF-Ratio was not increased due to contributions from free Zn.

In the absence of cells, HPLC stability analyses of Lom, oxATP and YM872 incubated for 30 min in the presence of H_2O_2, demonstrated that there was no effect of H_2O_2 on oxATP or YM872 stability, but lomerizine was degraded by approximately 15% (data not shown). Memantine could not be analysed due to the lack of a chromophore that could be detected by HPLC. Additionally, fluorescence detection of H_2O_2 indicated that H_2O_2 stability did not alter in the presence of each of the inhibitors, confirming a lack of a direct effect of the inhibitors on H_2O_2 and indicating that outcomes to be measured were due to effects of the inhibitors on cells.

The effects of all possible combinations of the Ca^{2+} channel inhibitors Lom, oxATP, YM872, and/or Mem on the intracellular Ca^{2+} concentration (ΔF-Ratio) of H_2O_2 stressed MC cells were assessed. The changes in Ca^{2+} concentration are expressed relative to the baseline Ca^{2+} concentration in the same culture before the addition of H_2O_2 and inhibitors. Ca^{2+} channel inhibitors were administered to cultures singly, in pairs, in groups of three or all four inhibitors, and ΔF-Ratios were compared to outcomes from H_2O_2 treated cultures without inhibitors. Of the single inhibitors, only oxATP significantly reduced ΔF-Ratio at 30 min ($df = 16$, $F = 20.78$; $p \leq 0.05$, Fig. 2A, Fig. 2B). Of the combinations of two inhibitors, only Lom + YM872, Lom + Mem, oxATP + YM872, and oxATP + Mem significantly reduced ΔF-Ratio ($df = 16$, $F = 20.78$, $p \leq 0.05$; Fig. 2A, Fig. 2C). The trend to an increased ΔF-Ratio with Mem + YM872 was not significant at any time point ($p > 0.05$). The finding that Lom + YM872 resulted in a significant reduction in ΔF-Ratio whereas YM872 alone did not, confirmed that the concentration of lomerizine used was sufficient to cause a biological effect despite some degradation in the presence of H_2O_2. Of the remaining combinations of three or four inhibitors, only Lom + oxATP + YM872, oxATP + YM872 + Mem, and Lom + oxATP + YM872 + Mem significantly reduced ΔF-Ratio ($df = 16$, $F = 20.78$, $p \leq 0.05$; Fig 2A, Fig. 2D). It is important to note that the apparently higher ΔF-Ratio following treatment with Lom + oxATP + Mem was not significantly different to the H_2O_2 control. This trend towards an anomalous finding was likely due to differences in ROI numbers between the two groups and the somewhat high variability observed with this inhibitor combination. Comparisons between ΔF-Ratios from MC cells treated with the various inhibitor combinations that reduced intracellular Ca^{2+} concentration relative to H_2O_2 without inhibitors, did not reveal significant differences between these inhibitor combinations at 30 min ($p > 0.05$, Fig 2A).

Differential reduction in cell viability with various Ca^{2+} channel inhibitor combinations

The association of acute changes in Ca^{2+} concentration with cell viability at 30 minutes as well as at later time points (i.e. 6, 24 h), was assessed in MC cells exposed to H_2O_2 insult. Following 30 min incubation with H_2O_2, the time point at which Ca^{2+} imaging was performed, there was no significant decrease in the percentage of viable cells relative to control (Fig. 3A, B). At 6 h, the percentage of live cells was significantly reduced, and remained significantly reduced at 24 h ($p \leq 0.05$, Fig. 3A, B) relative to control. The density of cells in control cultures was 1001.36 ± 70.18 cells/mm^2, was not significantly reduced at 30 min (1129.36 ± 84.92 cells/mm^2) but was significantly reduced at 6 (379.36 ± 54.51

cells/mm^2) and 24 h (405.08 ± 117.72 cells/mm^2, $p \leq 0.05$) relative to control (731.75 ± 93.75 and 658.73 ± 48.66 cells/mm^2 respectively).

The effects of Ca^{2+} channel inhibitor combinations on cell viability were assessed at 6 h; the choice of 6 h as opposed to 24 h was based upon the aim of assessing changes in viability associated with altered Ca^{2+} concentrations at 30 min, while minimising secondary effects likely to contribute to cell death at later time points. Of the fifteen Ca^{2+} channel inhibitor combinations, only seven combinations significantly increased the percentage of live cells compared to H_2O_2 control ($df = 16$, $F = 29.36$, $p \leq 0.05$). Specifically, of the single inhibitors, only oxATP significantly increased the percentage of viable cells ($p \leq 0.05$, Fig. 4). Note that reductions in intracellular Ca^{2+} concentration with single inhibitors (Fig. 2A, B) were directly associated with improvements in cell viability. Of the combinations of two inhibitors, only Lom + oxATP, oxATP + YM872, and oxATP + Mem significantly increased the percentage of live cells compared to H_2O_2 control ($p \leq 0.05$, Fig. 4). It is interesting to note that improvements in cell viability with treatment with Lom + oxATP were not associated with reduced intracellular Ca^{2+} concentration, whereas treatment with oxATP + YM872 and oxATP + Mem were associated both with reduced intracellular Ca^{2+} concentration (Fig. 2A, B) and improved viability. In contrast, Lom + YM872 and Lom + Mem treatments, which were observed to decrease intracellular Ca^{2+} concentration (Fig. 2A, B), had no effect on cell viability ($p > 0.05$, Fig. 4). Of the remaining combinations of three or four inhibitors, Lom + oxATP + YM872, Lom + oxATP + Mem, oxATP + YM872 + Mem, as well as Lom + oxATP + YM872 + Mem all significantly increased the percentage of viable cells ($p \leq 0.05$, Fig. 4). These improvements in cellular viability were directly associated with reductions in intracellular Ca^{2+} concentration for Lom + oxATP + YM872, oxATP + YM872 + Mem, and Lom + oxATP + YM872 + Mem treatments (Fig. 2A, B). However Lom + oxATP + Mem improved viability without altering intracellular Ca^{2+} concentration (Fig. 2A, 4). The effects of oxATP on viability in decreased extracellular Ca^{2+} concentrations were assessed using increasing concentrations of EGTA to chelate Ca^{2+}. The chosen EGTA concentrations have been shown to decrease extracellular Ca^{2+} concentration while maintaining cell viability (Takadera et al., 2010). EGTA alone had no significant effect on cell viability, and viability was significantly higher than H_2O_2 control at each of the tested concentrations ($df = 11$, $F = 23.90$; $p \leq 0.05$, Fig. 5). In the presence of H_2O_2, 1mM EGTA significantly increased cell viability compared to H_2O_2 control, indicating that increased extracellular Ca^{2+} contributes to H_2O_2 insult; lower EGTA concentrations had no significant effect. In contrast, in the presence

of oxATP, all tested concentrations of EGTA significantly increased cell viability compared to H_2O_2 control ($p \leq 0.05$, Fig. 5), which together with the demonstrated reduction of intracellular Ca^{2+} with oxATP (Fig. 2A), implies that the protective role of oxATP is Ca^{2+} dependent.

Increased viability of neurons, astrocytes, and NG2+ non-oligodendroglial cells with various Ca^{2+} channel inhibitor combinations

Early reductions in intracellular Ca^{2+} concentration were not always associated with improvements in cell viability at 6 h. It was therefore postulated that the Ca^{2+} channel inhibitor combinations may have differential effects on viabilities of specific cell sub-populations within the MC cultures. Accordingly, a selection of Ca^{2+} channel inhibitor combinations with a range of effects was used, and densities of individual cell sub-populations assessed. The Ca^{2+} channel inhibitor combinations tested were oxATP, Lom + oxATP, Lom + oxATP + Mem, Lom + oxATP + YM872, and Lom + oxATP + YM872 + Mem. Cell sub-populations were: β-III tubulin+ cells that are predominantly neurons (Katsetos et al., 1993); astrocytes (GFAP+); NG2+ non-oligodendroglial cells, likely to be predominantly pericytes and in some circumstances macrophages (Dimou and Gallo, 2015) (NG2+/Olig2-); oligodendroglia (Olig2+); and activated microglia/ macrophages (ED1+). The Olig2+ sub-population comprised approximately 70% Olig2+/NG2+ oligodendrocyte precursor cells; the remainder were Olig2+/NG2- and were therefore likely to be more mature oligodendrocytes. Following H_2O_2 insult in the absence of inhibitors, there was a statistically significant reduction in the density of β-III tubulin+, GFAP+, NG2+/Olig2-, Olig2+ and ED1+ cells, compared to control ($df = 7$, $F = 14.38, 4.82, 9.06, 22.95$, respectively, $p \leq 0.05$, Fig. 6~~5~~). In the presence of the six Ca^{2+} channel inhibitor combinations and H_2O_2, treatment with the five combinations that included oxATP resulted in significantly increased density of at least one of the cell sub-populations compared to the H_2O_2 only control ($p \leq 0.05$, Fig. 6~~5~~). However, no one inhibitor combination was uniformly effective. Specifically, H_2O_2 stressed cultures treated with Lom + oxATP + YM872 or Lom + oxATP + YM872 + Mem significantly increased the density of β-III tubulin+ cells ($p \leq 0.05$, Fig. 6~~5~~A, B). However, while the increases were significant, the degree of improvement was minor (Fig. 6~~5~~A). Only treatment with Lom + oxATP + YM872 + Mem resulted in significantly increased density of GFAP+ cells ($p \leq 0.05$, Fig. 6~~5~~C), with densities following all remaining treatments not significantly different from H_2O_2 only control ($p > 0.05$, Fig. 6~~5~~C, D). Treatment with oxATP, Lom + oxATP, Lom + oxATP + YM872, and Lom + oxATP + Mem significantly

increased the density of NG2+/Olig2- cells compared to H_2O_2 only control ($p \leq 0.05$, Fig. 6~~5~~E). However, only treatment with Lom + oxATP + YM872 and Lom + oxATP + Mem resulted in preservation of these NG2+/Olig2- cells to densities not significantly different to control ($p > 0.05$, Fig. 6E, F). No combinations of Ca^{2+} channel inhibitors were observed to have a significant effect on density of Olig2+ oligodendroglia or ED1+ microglia/ macrophages, compared to H_2O_2 only control ($p > 0.05$; Fig 6~~5~~ G-J).

Discussion

Using a high throughput *in vitro* model of CNS injury and multiple combinations of four Ca^{2+} channel inhibitors, we demonstrate that intracellular Ca^{2+} concentration is not always directly related to cell viability. Furthermore, while individual cell sub-populations were vulnerable to H_2O_2 insult, only some sub-populations could be rescued by treatment with Ca^{2+} channel inhibitors. Specifically, most Ca^{2+} channel inhibitor combinations including oxATP preserved NG2+ non-oligodendroglial cells, but preservation of astrocytes and neurons required additional inhibitors. $Olig2^{+}$ oligodendroglia and $ED\text{-}1^{+}$ activated microglia/ macrophages were not preserved by any of the inhibitor combinations.

Intracellular Ca^{2+} has been shown to be sequestered into mitochondria during excitotoxicity, triggering mitochondrial dysfunction and oxidative stress (Dykens, 1994; Lau and Tymianski, 2010). Reactive oxygen species (ROS) are generated as natural by-products of oxidative metabolism, and are vital for cell signaling and homeostasis (Kowaltowski et al., 2009b). However, exposure of mitochondria to increasing Ca^{2+} influx results in a secondary feed-forward mechanism whereby ROS production is enhanced (Dykens, 1994). This phenomenon has now been demonstrated for many cell types including neurons (Kahlert et al., 2005), cardiac myocytes (Viola et al., 2007) and vascular smooth muscle (Chaplin et al., 2015). Excess ROS can spread, leading to oxidative damage *in vivo* (Kowaltowski et al., 2009b; Fitzgerald et al., 2010b). Following injury to the central nervous system, infiltrating inflammatory cells that enter the injury site are a significant additional source of ROS, including H_2O_2 (O'Hare Doig et al., 2014b). Multiple feed forward mechanisms that result in ROS initiate further increases in intracellular Ca^{2+} levels, contributing to additional cell death (Kristian and Siesjo, 1998). Proposed mechanisms by which H_2O_2 causes increased intracellular Ca^{2+} levels include activation of VGCCs (Roveri et al., 1992), nonspecific changes in membrane permeability to Ca^{2+} (Rojanasakul et al., 1993), changes in the Na^{+}-Ca^{2+} exchanger (Kaneko et al., 1989), and H_2O_2 induced Ca^{2+} release from intracellular stores (Nicotera and Rossi, 1994). Our data indicate that both release of Ca^{2+} from ryanodine sensitive intracellular stores and influx of extracellular Ca^{2+} through $P2X_7R$ as well as other Ca^{2+} channels contribute to the rise in intracellular Ca^{2+} levels following H_2O_2 insult.

Given the consequences of excessive Ca^{2+} entry into neurons and glia following injury, it was hypothesized that reductions in intracellular Ca^{2+} levels following treatment with Ca^{2+} channel inhibitors would be associated with increased cell viability. Reductions in

intracellular Ca^{2+} concentration with oxATP treatment were directly associated with substantial improvements in cell viability. However, treatment with the inhibitor combinations Lom + oxATP, Lom + YM872 and Lom + Mem revealed that dissociation between intracellular Ca^{2+} concentration and cell viability can occur in this model system. Thus, one cannot simply assume that intracellular Ca^{2+} overload results in cell death. As cell viability was increased following treatment with all combinations of inhibitors that included oxATP, the results indicate that controlling intracellular Ca^{2+} concentration by limiting influx *via* P_2X_7Rs may play an important role in maintaining cortical cell viability *in vitro* following insult. As such, the data support the '*source specificity hypothesis*' whereby Ca^{2+} cytotoxicity is not merely a function of increased Ca^{2+} concentration, but instead is linked to specific second messenger pathways activated by excessive Ca^{2+} entry through specific channels (Tymianski et al., 1993). Interestingly however, treatment with Lom + YM872 or Lom + Mem were not protective, and nor were YM872 or Mem alone. Furthermore, almost all combinations of Ca^{2+} channel inhibitors that included both YM872 + Mem were not protective: exceptions were treatments that included oxATP. While somewhat speculative at this stage, it is possible that Ca^{2+} influx through both Ca^{2+} permeable AMPAR and/ or NMDAR is necessary for MC cell health following H_2O_2 insult, and that the cytotoxic consequences of excessive Ca^{2+} through these channels can be overcome by the inhibitory action of oxATP on P_2X_7Rs and subsequent downstream events. Inhibition of flux of other ions through Ca^{2+} permeable AMPAR, P_2X_7Rs and NMDAR may also influence viability.

The apparent dissociation between intracellular Ca^{2+} concentration and MC cell viability may have been due to masking of differential effects on individual cell sub-populations by the effects on the mixed cell population as a whole. Ca^{2+} imaging studies on pure neuronal and/or astrocyte cultures exposed to H_2O_2 stress and the multiple combinations of Ca^{2+} channel inhibitors were considered, however such studies would ignore the complexities of inter-cellular interactions, cytokine release in response to stress and inter-cellular transfer of reactive species via gap junctions. Increase in intracellular Ca^{2+} concentration in neurons *via* P_2X_7R ion channels plays a major role in mitochondrial dysfunction leading to apoptotic neuronal death (Nishida et al., 2012). However, treatment with oxATP was insufficient to protect neuronal density. Reports have indicated that neurons are particularly sensitive to H_2O_2 (Behl et al., 1994; Whittemore et al., 1994). Thus, it is likely that the 6 h H_2O_2 insult overwhelmed the protective effect of oxATP and additional inhibitors were required for even minimal neuroprotection. While there was a trend to protection of astrocytes by most of the

tested combinations of Ca^{2+} channel inhibitors, only the combination of all four inhibitors resulted in significant protection. Astrocytes release glutamate and ATP in the injured scenario *via* a number of mechanisms (Bal-Price et al., 2002; Ye et al., 2003) including $P2X_7Rs$ (Duan et al., 2003) and this can have detrimental effects on adjacent cells. The loss of astrocytes despite treatment with most inhibitor combinations may have limited their contribution to damage to surrounding cell sub-populations. NG2-glia are an abundant population of cells in the adult CNS that can generate multiple cell types including oligodendrocytes, type 2-astrocytes and pericytes (Richardson et al., 2011). NG2-glia have been shown to evoke increased intracellular Ca^{2+} concentrations in optic nerves *in situ* following $P2X_7R$ and AMPAR activation, with ATP alone evoking robust changes in intracellular Ca^{2+} (Hamilton et al., 2010). In the current study, inhibition of $P2X_7R$ with oxATP resulted in increased NG2-glia viability. However, protection was only observed for NG2+ cells that were not of an oligodendroglial lineage. Olig2+ oligodendroglia, were approximately 70% oligodendrocyte precursor cells, and not protected by any of the Ca^{2+} inhibitor combinations, likely reflecting the known selective vulnerability of OPCs to oxidative stress (Back et al., 1998). Despite a lack of protection of oligodendroglia by the tested inhibitor combinations *in vitro,* Lom treatment has been shown to preserve myelin compaction in vulnerable white matter following partial optic nerve transection *in vivo,* and short term delivery of oxATP + YM872 together with sustained delivery of Lom preserved node/paranode structure as well as visual function in this *in vivo* model (Savigni et al., 2013). These data indicate that the three Ca^{2+} channel inhibitors in combination have a beneficial effect on oligodendroglia *in vivo*. While the MC cells utilized in the current study contain many of the cell types found *in vivo,* three dimensional architecture and cellular interactions are lacking. It is increasingly understood that NG2-glia are required at the Node of Ranvier for axonal and myelin integrity (Butt et al., 1999). Our demonstration of protection of NG2+/olig2- cells by combinations of ion channels containing oxATP indicate that protection of these particular cells may be a critical element preserving structure and function of intact but vulnerable myelinated axons of the CNS *in vivo*.

Conclusions

The contribution of specific Ca^{2+} channels to excess Ca^{2+} influx in individual cell sub-populations in this *in vitro* model may not reflect the complexities of the injured CNS. Nevertheless, the data provide insight into effects of inhibition of individual and multiple

Ca^{2+} channels on cell sub-populations, with a breadth and scope not feasible in *in vivo* studies. The demonstration of protection of MC viability with oxATP alone and in combination with other Ca^{2+} channel inhibitors provides support for further *in vivo* investigation where the presence of oxATP is maintained long term after CNS injury.

Acknowledgements

We acknowledge financial support from the Neurotrauma Research Program of Western Australia, an initiative of the Road Safety Council of Western Australia. This project is funded through the Road Trauma Trust Account, Western Australia, but does not reflect views or recommendations of the Road Safety Council. We thank Dr Robert Gasperini for his helpful advice on Ca^{2+} imaging. MF is supported by an NHMRC Career Development Fellowship (APP1087114).

Figure Legends

Figure 1. Hydrogen peroxide insult increases intracellular Ca^{2+} in MC cells via intracellular and extracellular sources. Representative images show increased Fura340 fluorescence (blue) at 30 min in MC cells stressed with H_2O_2 (A); scale bar = 20µm. Quantification of ΔF-Ratio through analysis of Fura-2 AM emissions under 340/380 nm excitation, immediately preceding and following 400µm H_2O_2 insult, traces of mean data over time are shown (B): 3-4 separate experiments were conducted for each data point, encompassing a total of 27-40 cells/ treatment group. MC cells treated with H_2O_2 ± ryanodine (10µm, 20µm or 40µm) for 30 min, traces of mean data shown (B): 3-4 separate experiments encompassing a total of 10-20 cells/ treatment group. ΔF-Ratio in MC cells treated with H_2O_2 ± TPEN (1µm or 10µm) for 30 min, traces of mean data shown (D): 3-4 separate experiments were conducted, encompassing a total of 10-20 cells/ treatment group; note that the colouring of traces for control and H_2O_2 are represented using the same colours as in B.

Figure 2. Various combinations of Ca^{2+} channel inhibitors reduce the intracellular Ca^{2+} concentration of MC cells following H_2O_2 insult. ΔF-Ratios derived from Fura-2 AM emissions under 340/380 nm excitation immediately preceding and following 400µm H_2O_2 insult ± Ca^{2+} channel inhibitors at 30 min (A): 4-5 separate experiments were conducted, encompassing a total of 14-40 cells/ treatment group; * statistically significantly different from H_2O_2, $p \leq 0.05$. Note that while all control values at 0 min approach 1.0, they are not identical. Traces of mean ΔF-Ratios throughout the 30 min incubation period are shown for MC cells treated with single inhibitors (B), pairs of inhibitors (C) or three or 4 inhibitors in combination (D); note that the colouring of traces for control and H_2O_2 in C and D are represented using the same colours as in B.

Figure 3. Time dependent changes in MC cell viability with H_2O_2 insult. Mean ± SEM percent viable MC cells following incubation with 400µm H_2O_2 for 30 min, 6 or 24 h compared to control at each time point (A): * statistically significantly different from control at each time point, $p \leq 0.05$. Representative images of MC cells stained with Calcein-AM and Ethidium homodimer following incubation with 400µm H_2O_2 are shown (B), scale bar = 75µm.

Figure 4. Treatment with various combinations of Ca^{2+} channel inhibitors increases viability of MC cells following H_2O_2 insult. Mean ± SEM percent viable MC cells following incubation with 400µm H_2O_2 ± combinations of Ca^{2+} channel inhibitors for 6 h; * statistically significantly different from H_2O_2 only control, $p \leq 0.05$.

Figure 5. Effects of the Ca^{2+} chelator EGTA on MC viability in the presence of oxATP and H_2O_2 insult. Mean ± SEM percent viable MC cells following incubation with 400µm H_2O_2 ± oxATP, with or without increasing concentrations of EGTA for 6 h; * statistically significantly different from H_2O_2 only control, $p \leq 0.05$.

Figure 6~~5~~. Treatment with various combinations of Ca^{2+} channel inhibitors increases viability of specific cell sub-populations. Mean ± SEM density (/mm^2) of βIII tubulin+ neurons (A), GFAP+ astrocytes (C), NG2+/Olig2- NG2+ non-oligodendroglial cells (E), Olig2+ oligodendroglia (G), and ED1+ activated microglia/macrophages (I) following incubation with 400µm H_2O_2 ± Ca^{2+} channel inhibitors for 6 h compared to control; * statistically significantly different from H_2O_2 only control, $p \leq 0.05$. Representative images of βIII tubulin+ neurons (green) (B), GFAP+ astrocytes (red) (D), NG2+ (green) /olig2- non oligodendroglial cells (F), Olig2+ (red) oligodendroglia (H) and ED1+ microglia/ macrophages (green) (J) are shown; all with Hoechst nuclear stain, scale bar = 100µm.

References

Agrawal SK, Nashmi R, Fehlings MG (2000) Role of L- and N-type calcium channels in the pathophysiology of traumatic spinal cord white matter injury. Neuroscience 99:179-188.

Back SA, Gan X, Li Y, Rosenberg PA, Volpe JJ (1998) Maturation-dependent vulnerability of oligodendrocytes to oxidative stress-induced death caused by glutathione depletion. Journal of Neuroscience 18:6241-6253.

Bal-Price A, Moneer Z, Brown GC (2002) Nitric oxide induces rapid, calcium-dependent release of vesicular glutamate and ATP from cultured rat astrocytes. Glia 40:312-323.

Baraldi PG, Romagnoli R, Tabrizi MA, Falzoni S, di Virgilio F (2000) Synthesis of conformationally constrained analogues of KN62, a potent antagonist of the P2X7-receptor. Bioorg Med Chem Lett 10:681-684.

Baraldi PG, del Carmen Nunez M, Morelli A, Falzoni S, Di Virgilio F, Romagnoli R (2003) Synthesis and biological activity of N-arylpiperazine-modified analogues of KN-62, a potent antagonist of the purinergic P2X7 receptor. J Med Chem 46:1318-1329.

Baraldi PG, Makaeva R, Pavani MG, Nunez Mdel C, Spalluto G, Moro S, Falzoni S, Di Virgilio F, Romagnoli R (2002) Synthesis, biological activity and molecular modeling studies of 1,2,3,4-tetrahydroisoquinoline derivatives as conformationally constrained analogues of KN62, a potent antagonist of the P2X7-receptor containing a tyrosine moiety. Arzneim-Forsch 52:273-285.

Behl C, Davis JB, Lesley R, Schubert D (1994) Hydrogen peroxide mediates amyloid beta protein toxicity. Cell 77:817-827.

Block F, Schwarz M (1996) Memantine reduces functional and morphological consequences induced by global ischemia in rats. Neuroscience letters 208:41-44.

Bolanos JP, Almeida A, Stewart V, Peuchen S, Land JM, Clark JB, Heales SJ (1997) Nitric oxide-mediated mitochondrial damage in the brain: mechanisms and implications for neurodegenerative diseases. J Neurochem 68:2227-2240.

Braughler JM, Hall ED (1992) Involvement of lipid peroxidation in CNS injury. J Neurotrauma 9 Suppl 1:S1-7.

Butt AM, Duncan A, Hornby MF, Kirvell SL, Hunter A, Levine JM, Berry M (1999) Cells expressing the NG2 antigen contact nodes of Ranvier in adult CNS white matter. Glia 26:84-91.

Camello-Almaraz MC, Pozo MJ, Murphy MP, Camello PJ (2006) Mitochondrial production of oxidants is necessary for physiological calcium oscillations. J Cell Physiol 206:487-494.

Chaplin NL, Nieves-Cintron M, Fresquez AM, Navedo MF, Amberg GC (2015) Arterial Smooth Muscle Mitochondria Amplify Hydrogen Peroxide Microdomains Functionally Coupled to L-Type Calcium Channels. Circ Res.

Cornelius C, Crupi R, Calabrese V, Graziano A, Milone P, Pennisi G, Radak Z, Calabrese EJ, Cuzzocrea S (2013) Traumatic brain injury: oxidative stress and neuroprotection. Antioxid Redox Signal 19:836-853.

Dimou L, Gallo V (2015) NG2-glia and their functions in the central nervous system. Glia 63:1429-1451.

Doble A (1999) The role of excitotoxicity in neurodegenerative disease: implications for therapy. Pharmacology & therapeutics 81:163-221.

Duan S, Anderson CM, Keung EC, Chen Y, Chen Y, Swanson RA (2003) P2X7 receptor-mediated release of excitatory amino acids from astrocytes. The Journal of neuroscience : the official journal of the Society for Neuroscience 23:1320-1328.

Dykens JA (1994) Isolated cerebral and cerebellar mitochondria produce free radicals when exposed to elevated CA2+ and Na+: implications for neurodegeneration. Journal of neurochemistry 63:584-591.

Ehrlich M, Knolle E, Ciovica R, Bock P, Turkof E, Grabenwoger M, Cartes-Zumelzu F, Kocher A, Pockberger H, Fang WC, Wolner E, Havel M (1999) Memantine for prevention of spinal cord injury in a rabbit model. The Journal of thoracic and cardiovascular surgery 117:285-291.

Fawcett JW, Asher RA (1999) The glial scar and central nervous system repair. Brain Res Bull 49:377-391.

Fehlings MG, Tator CH, Linden RD (1989) The effect of nimodipine and dextran on axonal function and blood flow following experimental spinal cord injury. J Neurosurg 71:403-416.

Fitzgerald M, Bartlett CA, Harvey AR, Dunlop SA (2010a) Early events of secondary degeneration after partial optic nerve transection: an immunohistochemical study. J Neurotrauma 27:439-452.

Fitzgerald M, Bartlett CA, Harvey AR, Dunlop SA (2010b) Early events of secondary degeneration after partial optic nerve transection: an immunohistochemical study. J Neurotrauma 27:439-452.

Fitzgerald M, Payne SC, Bartlett CA, Evill L, Harvey AR, Dunlop SA (2009) Secondary retinal ganglion cell death and the neuroprotective effects of the calcium channel blocker lomerizine. Invest Ophthalmol Vis Sci 50:5456-5462.

Follett PL, Rosenberg PA, Volpe JJ, Jensen FE (2000) NBQX attenuates excitotoxic injury in developing white matter. Journal of Neuroscience 20:9235-9241.

Gandhi S, Wood-Kaczmar A, Yao Z, Plun-Favreau H, Deas E, Klupsch K, Downward J, Latchman DS, Tabrizi SJ, Wood NW, Duchen MR, Abramov AY (2009) PINK1-associated Parkinson's disease is caused by neuronal vulnerability to calcium-induced cell death. Molecular cell 33:627-638.

Gill R (1994) The pharmacology of alpha-amino-3-hydroxy-5-methyl-4-isoxazole propionate (AMPA)/kainate antagonists and their role in cerebral ischaemia. Cerebrovascular and brain metabolism reviews 6:225-256.

Gomez TM, Spitzer NC (2000) Regulation of growth cone behavior by calcium: new dynamics to earlier perspectives. J Neurobiol 44:174-183.

Graham SH, Chen J, Lan JQ, Simon RP (1996) A dose-response study of neuroprotection using the AMPA antagonist NBQX in rat focal cerebral ischemia. J Pharmacol Exp Ther 276:1-4.

Grynkiewicz G, Poenie M, Tsien RY (1985) A new generation of Ca2+ indicators with greatly improved fluorescence properties. J Biol Chem 260:3440-3450.

Hamilton N, Vayro S, Wigley R, Butt AM (2010) Axons and astrocytes release ATP and glutamate to evoke calcium signals in NG2-glia. Glia 58:66-79.

Hara H, Shimazawa M, Sasaoka M, Yamada C, Iwakura Y, Sakai T, Maeda Y, Yamaguchi T, Sukamoto T, Hashimoto M (1999) Selective effects of lomerizine, a novel diphenylmethylpiperazine Ca2+ channel blocker, on cerebral blood flow in rats and dogs. Clinical and experimental pharmacology & physiology 26:870-876.

Haskew-Layton RE, Payappilly JB, Smirnova NA, Ma TC, Chan KK, Murphy TH, Guo H, Langley B, Sultana R, Butterfield DA, Santagata S, Alldred MJ, Gazaryan IG, Bell GW, Ginsberg SD, Ratan RR (2010) Controlled enzymatic production of astrocytic hydrogen peroxide protects neurons from oxidative stress via an Nrf2-independent pathway. Proc Natl Acad Sci U S A 107:17385-17390.

Hausmann ON (2003) Post-traumatic inflammation following spinal cord injury. Spinal cord 41:369-378.

Herson PS, Lee K, Pinnock RD, Hughes J, Ashford ML (1999) Hydrogen peroxide induces intracellular calcium overload by activation of a non-selective cation channel in an insulin-secreting cell line. The Journal of biological chemistry 274:833-841.

Hollmann M, Hartley M, Heinemann S (1991) Ca2+ permeability of KA-AMPA--gated glutamate receptor channels depends on subunit composition. Science 252:851-853.

Huang CY, Wang LC, Wang HK, Pan CH, Cheng YY, Shan YS, Chio CC, Tsai KJ (2015) Memantine alleviates brain injury and neurobehavioral deficits after experimental subarachnoid hemorrhage. Mol Neurobiol 51:1038-1052.

Huang X, Li Q, Li H, Guo L (2009) Neuroprotective and antioxidative effect of cactus polysaccharides in vivo and in vitro. Cell Mol Neurobiol 29:1211-1221.

Kahlert S, Zundorf G, Reiser G (2005) Glutamate-mediated influx of extracellular Ca2+ is coupled with reactive oxygen species generation in cultured hippocampal neurons but not in astrocytes. Journal of neuroscience research 79:262-271.

Kaneko M, Beamish RE, Dhalla NS (1989) Depression of heart sarcolemmal Ca2+-pump activity by oxygen free radicals. Am J Physiol Heart Circ Physiol 256:H368-H374.

Katsetos CD, Frankfurter A, Christakos S, Mancall EL, Vlachos IN, Urich H (1993) Differential localization of class III, beta-tubulin isotype and calbindin-D28k defines distinct neuronal types in the developing human cerebellar cortex. Journal of neuropathology and experimental neurology 52:655-666.

Kerschensteiner M, Schwab ME, Lichtman JW, Misgeld T (2005) In vivo imaging of axonal degeneration and regeneration in the injured spinal cord. Nat Med 11:572-577.

Klein KU, Engelhard K (2010) Perioperative neuroprotection. Best practice & research Clinical anaesthesiology 24:535-549.

Komuro H, Rakic P (1996) Intracellular Ca2+ fluctuations modulate the rate of neuronal migration. Neuron 17:275-285.

Kowaltowski AJ, de Souza-Pinto NC, Castilho RF, Vercesi AE (2009a) Mitochondria and reactive oxygen species. Free Radic Biol Med 47:333-343.

Kowaltowski AJ, de Souza-Pinto NC, Castilho RF, Vercesi AE (2009b) Mitochondria and reactive oxygen species. Free Radic Biol Med 47:333-343.

Kristian T, Siesjo BK (1998) Calcium in ischemic cell death. Stroke 29:705-718.

Lau A, Tymianski M (2010) Glutamate receptors, neurotoxicity and neurodegeneration. European journal of physiology 460:525-542.

Lipton P (1999) Ischemic cell death in brain neurons. Physiol Rev 79:1431-1568.

Liu XZ, Xu XM, Hu R, Du C, Zhang SX, McDonald JW, Dong HX, Wu YJ, Fan GS, Jacquin MF, Hsu CY, Choi DW (1997) Neuronal and glial apoptosis after traumatic spinal cord injury. Journal of Neuroscience 17:5395-5406.

Ma S, Liu H, Jiao H, Wang L, Chen L, Liang J, Zhao M, Zhang X (2012) Neuroprotective effect of ginkgolide K on glutamate-induced cytotoxicity in PC 12 cells via inhibition of ROS generation and Ca(2+) influx. Neurotoxicology 33:59-69.

Mandavilli BS, Boldogh I, Van Houten B (2005) 3-nitropropionic acid-induced hydrogen peroxide, mitochondrial DNA damage, and cell death are attenuated by Bcl-2 overexpression in PC12 cells. Brain research Molecular brain research 133:215-223.

Matute C (2006) Oligodendrocyte NMDA receptors: a novel therapeutic target. Trends Mol Med 12:289-292.

Matute C, Domercq M, Sanchez-Gomez MV (2006) Glutamate-mediated glial injury: mechanisms and clinical importance. Glia 53:212-224.

Matute C, Sanchez-Gomez MV, Martinez-Millan L, Miledi R (1997) Glutamate receptor-mediated toxicity in optic nerve oligodendrocytes. Proc Natl Acad Sci U S A 94:8830-8835.

Matute C, Torre I, Perez-Cerda F, Perez-Samartin A, Alberdi E, Etxebarria E, Arranz AM, Ravid R, Rodriguez-Antiguedad A, Sanchez-Gomez M, Domercq M (2007) P2X(7) receptor blockade prevents ATP excitotoxicity in oligodendrocytes and ameliorates experimental autoimmune encephalomyelitis. Journal of Neuroscience 27:9525-9533.

McAllister J, Ghosh S, Berry D, Park M, Sadeghi S, Wang KX, Parker WD, Swerdlow RH (2008) Effects of memantine on mitochondrial function. Biochemical pharmacology 75:956-964.

Muralidharan P, Cserne Szappanos H, Ingley E, Hool L (2016) Evidence for redox sensing by a human cardiac calcium channel. Sci Rep 6:19067.

Neary JT, Kang Y, Tran M, Feld J (2005) Traumatic injury activates protein kinase B/Akt in cultured astrocytes: role of extracellular ATP and P2 purinergic receptors. J Neurotrauma 22:491-500.

Nicotera P, Rossi A (1994) Nuclear Ca2+: physiological regulation and role in apoptosis. Mol Cell Biochem 135:89-98.

Nishida K, Nakatani T, Ohishi A, Okuda H, Higashi Y, Matsuo T, Fujimoto S, Nagasawa K (2012) Mitochondrial dysfunction is involved in P2X7 receptor-mediated neuronal cell death. Journal of neurochemistry 122:1118-1128.

O'Hare Doig RL, Bartlett CA, Maghzal GJ, Lam M, Archer M, Stocker R, Fitzgerald M (2014a) Reactive species and oxidative stress in optic nerve vulnerable to secondary degeneration. Exp Neurol 261C:136-146.

O'Hare Doig RL, Bartlett CA, Maghzal GJ, Lam M, Archer M, Stocker R, Fitzgerald M (2014b) Reactive species and oxidative stress in optic nerve vulnerable to secondary degeneration. Exp Neurol 261:136-146.

Ouardouz M, Nikolaeva MA, Coderre E, Zamponi GW, McRory JE, Trapp BD, Yin X, Wang W, Woulfe J, Stys PK (2003) Depolarization-induced Ca2+ release in ischemic spinal cord white matter involves L-type Ca2+ channel activation of ryanodine receptors. Neuron 40:53-63.

Payne SC, Bartlett CA, Harvey AR, Dunlop SA, Fitzgerald M (2011) Chronic swelling and abnormal myelination during secondary degeneration after partial injury to a central nervous system tract. J Neurotrauma 28:1077-1088.

Prilloff S, Noblejas MI, Chedhomme V, Sabel BA (2007) Two faces of calcium activation after optic nerve trauma: life or death of retinal ganglion cells in vivo depends on calcium dynamics. Eur J Neurosci 25:3339-3346.

Richardson WD, Young KM, Tripathi RB, McKenzie I (2011) NG2-glia as multipotent neural stem cells: fact or fantasy? Neuron 70:661-673.

Rojanasakul Y, Wang L, Hoffman AH, Shi X, Dalal NS, Banks DE, Ma JKH (1993) Mechanisms of Hydroxyl Free Radical-induced Cellular Injury and Calcium Overloading in Alveolar Macrophages. Am J Respir Cell Mol Biol 8:377-383.

Roveri A, Coassin M, Maiorino M, Zamburlini A, van Amsterdam FTM, Ratti E, Ursini F (1992) Effect of hydrogen peroxide on calcium homeostasis in smooth muscle cells. Arch Biochem Biophys 297:265-270.

Savigni DL, O'Hare Doig RL, Szymanski CR, Bartlett CA, Lozic I, Smith NM, Fitzgerald M (2013) Three Ca2+ channel inhibitors in combination limit chronic secondary degeneration following neurotrauma. Neuropharmacology 75:380-390.

Spitzer NC, Lautermilch NJ, Smith RD, Gomez TM (2000) Coding of neuronal differentiation by calcium transients. BioEssays 22:811-817.

Stack EC, Smith KM, Ryu H, Cormier K, Chen M, Hagerty SW, Del Signore SJ, Cudkowicz ME, Friedlander RM, Ferrante RJ (2006) Combination therapy using minocycline and coenzyme Q10 in R6/2 transgenic Huntington's disease mice. Biochim Biophys Acta 1762:373-380.

Suadicani SO, Cherkas PS, Zuckerman J, Smith DN, Spray DC, Hanani M (2010) Bidirectional calcium signaling between satellite glial cells and neurons in cultured mouse trigeminal ganglia. Neuron Glia Biol 6:43-51.

Szymanski CR, Chiha W, Morellini N, Cummins N, Bartlett CA, O'Hare Doig RL, Savigni DL, Payne SC, Harvey AR, Dunlop SA, Fitzgerald M (2013) Paranode abnormalities and oxidative stress in optic nerve vulnerable to secondary degeneration: modulation by 670 nm light treatment. PLoS One 8:e66448.

Takadera T, Ohtsuka M, Aoki H (2010) Chelation of extracellular calcium-induced cell death was prevented by glycogen synthase kinase-3 inhibitors in PC12 cells. Cell Mol Neurobiol 30:193-198.

Takahashi M, Ni JW, Kawasaki-Yatsugi S, Toya T, Ichiki C, Yatsugi SI, Koshiya K, Shimizu-Sasamata M, Yamaguchi T (1998) Neuroprotective efficacy of YM872, an alpha-amino-3-hydroxy-5-methylisoxazole-4-propionic acid receptor antagonist, after permanent middle cerebral artery occlusion in rats. J Pharmacol Exp Ther 287:559-566.

Tamaki Y, Araie M, Fukaya Y, Nagahara M, Imamura A, Honda M, Obata R, Tomita K (2003) Effects of lomerizine, a calcium channel antagonist, on retinal and optic nerve head circulation in rabbits and humans. Invest Ophthalmol Vis Sci 44:4864-4871.

Tanaka T, Nangaku M, Miyata T, Inagi R, Ohse T, Ingelfinger JR, Fujita T (2004) Blockade of calcium influx through L-type calcium channels attenuates mitochondrial injury and apoptosis in hypoxic renal tubular cells. J Am Soc Nephrol 15:2320-2333.

Tekkok SB, Goldberg MP (2001) Ampa/kainate receptor activation mediates hypoxic oligodendrocyte death and axonal injury in cerebral white matter. Journal of Neuroscience 21:4237-4248.

Totoiu MO, Keirstead HS (2005) Spinal cord injury is accompanied by chronic progressive demyelination. J Comp Neurol 486:373-383.

Tuszynski MH (2005) New strategies for CNS repair. Ernst Schering Res Found Workshop:1-10.

Tymianski M, Charlton MP, Carlen PL, Tator CH (1993) Source specificity of early calcium neurotoxicity in cultured embryonic spinal neurons. Journal of Neuroscience 13:2085-2104.

van den Pol AN, Finkbeiner SM, Cornell-Bell AH (1992) Calcium excitability and oscillations in suprachiasmatic nucleus neurons and glia in vitro. J Neurosci 12:2648-2664.

Viola HM, Arthur PG, Hool LC (2007) Transient exposure to hydrogen peroxide causes an increase in mitochondria-derived superoxide as a result of sustained alteration in L-type Ca2+ channel function in the absence of apoptosis in ventricular myocytes. Circ Res 100:1036-1044.

Wang X, Arcuino G, Takano T, Lin J, Peng WG, Wan P, Li P, Xu Q, Liu QS, Goldman SA, Nedergaard M (2004) P2X7 receptor inhibition improves recovery after spinal cord injury. Nat Med 10:821-827.

Weishaupt N, Silasi G, Colbourne F, Fouad K (2010) Secondary damage in the spinal cord after motor cortex injury in rats. J Neurotrauma 27:1387-1397.

Whittemore ER, Loo DT, Cotman CW (1994) Exposure to hydrogen peroxide induces cell death via apoptosis in cultured rat cortical neurons. Neuroreport 5:1485-1488.

Xue D, Huang ZG, Barnes K, Lesiuk HJ, Smith KE, Buchan AM (1994) Delayed treatment with AMPA, but not NMDA, antagonists reduces neocortical infarction. Journal of Cerebral Blood Flow and Metabolism 14:251-261.

Ye ZC, Wyeth MS, Baltan-Tekkok S, Ransom BR (2003) Functional hemichannels in astrocytes: a novel mechanism of glutamate release. The Journal of neuroscience : the official journal of the Society for Neuroscience 23:3588-3596.

Zhang Z, He Y, Tuteja D, Xu D, Timofeyev V, Zhang Q, Glatter KA, Xu Y, Shin HS, Low R, Chiamvimonvat N (2005) Functional roles of Cav1.3(alpha1D) calcium channels in atria: insights gained from gene-targeted null mutant mice. Circulation 112:1936-1944.

Specific combinations of Ca^{2+} channel inhibitors reduce excessive Ca^{2+} influx as a consequence of oxidative stress and increase neuronal and glial cell viability *in vitro*

Ryan L. O'Hare Doig,[1,2,3] Carole A. Bartlett,[1,2] Nicole M. Smith, [1,2, 4] Stuart I. Hodgetts,[1,3] Sarah A. Dunlop,[1,2] Livia Hool,[3,5] and Melinda Fitzgerald[1,2]

[1]Experimental and Regenerative Neurosciences, [2]School of Animal Biology, [3]School of Anatomy, Physiology and Human Biology, [4]School of Chemistry and Biochemistry, The University of Western Australia, Crawley, Western Australia, Australia, [5]Victor Chang Cardiac Research Institute, Sydney, New South Wales, Australia

Corresponding Author: Melinda Fitzgerald - lindy.fitzgerald@uwa.edu.au

Experimental and Regenerative Neurosciences, School of Animal Biology, The University of Western Australia, Crawley, 6009 Western Australia, Australia

Phone: 61 8 6488 2353

Highlights *(note, these are limited to 85 characters each)*

The effects of combinations of Ca^{2+} channel inhibitors on H_2O_2 stressed cells were assessed *in vitro.*

Most combinations of inhibitors with oxATP decreased Ca^{2+} influx and increased cell viability.

However, reductions in intracellular Ca^{2+} concentration were not always linked to cell viability.

Combinations of inhibitors preserved some cell subpopulations, particularly NG2+/olig2- glia.

The data increase understanding of the efficacy of Ca^{2+} channel inhibitor combinations *in vivo*

Abstract

Combinations of Ca^{2+} channel inhibitors have been proposed as an effective means to prevent excess Ca^{2+} flux and death of neurons and glia following neurotrauma *in vivo*. However, it is not yet known if beneficial outcomes such as improved viability have been due to direct effects on intracellular Ca^{2+} concentrations. Here, the effects of combinations of Lomerizine (Lom), YM872, memantine and/or oxATP to block voltage gated Ca^{2+} channels, Ca^{2+} permeable AMPA receptors, NMDA receptors and purinergic $P2X_7$ receptors ($P2X_7R$) respectively, on Ca^{2+} concentration and viability of primary mixed cortical cultures exposed to hydrogen peroxide (H_2O_2) insult, were assessed. The contribution of Ryanodine sensitive intracellular stores to intracellular Ca^{2+} concentration was also assessed. Live cell calcium imaging revealed that a 30 minute H_2O_2 insult induced a slow increase in intracellular Ca^{2+}, in part from intracellular sources, associated with loss of cell viability by 6 hours. Most combinations of inhibitors that included oxATP significantly decreased Ca^{2+} influx and increased cell viability when administered simultaneously with H_2O_2. However, reductions in intracellular Ca^{2+} concentration were not always linked to improved cell viability. Examination of the density of specific cell subpopulations demonstrated that most combinations of inhibitors that included oxATP preserved NG2+ non-oligodendroglial cells, but preservation of astrocytes and neurons required additional inhibitors. $Olig2^+$ oligodendroglia and $ED\text{-}1^+$ activated microglia/macrophages were not preserved by any of the inhibitor combinations. These data indicate that following H_2O_2 insult, limiting intracellular Ca^{2+} entry *via* $P2X_7R$ is generally associated with increased cell viability. Protection of NG2+ non-oligodendroglial cells by Ca^{2+} channel inhibitor combinations may contribute to observed beneficial outcomes *in vivo*.

Keywords

Ca^{2+} channel inhibitors; intracellular Ca^{2+} concentration; oligodendroglia; NG2-glia; cell viability

Abbreviations

AMPA, α-amino-3-hydroxy-5-methyl-4-isoxazolepropionic acid; AMPARs, α-amino-3-hydroxy-5-methyl-4-isoxazolepropionic acid receptors; ANOVA, analysis of variance; ATP, adenosine 5'-triphosphate; Ca^{2+}, calcium; CNS, central nervous system; DMSO, dimethyl sulfoxide; FOV, field of view; HBSS, Hanks balanced salt solution; h, hours; Lom, Lomerizine; MC, mixed cortical; Memantine (Mem), 3,5-dimethyl-1-adamantanamine; min, minutes; NB, Neurobasal® medium; NMDA, *N*-methyl-D-aspartate; NMDARs, *N*-methyl-D-aspartate receptors; oxATP, adenosine 5'-triphosphate periodate oxidized sodium salt; PFA, paraformaldehyde; PBS, phosphate buffered saline; PVG, Piebald Viral Glaxo; $P2X_7R$, $P2X_7$ receptors; ROI, region of interest; SCI, spinal cord injury; SEM, standard error of the mean; VGCCs, voltage-gated Ca^{2+} channels; YM872, 2,3-dioxo-7-(1*H*-imidazol-1-yl)6-nitro-1,2,3,4-tetrahydro-1-quinoxalinyl]acetic acid monohydrate;

Introduction

In the CNS, calcium (Ca^{2+}) plays a vital role in important physiological processes such as cell differentiation, growth and survival (Komuro and Rakic, 1996; Gomez and Spitzer, 2000; Spitzer et al., 2000). Changes in cytosolic Ca^{2+} stimulate multiple Ca^{2+}-dependent pathways, normally designed to maintain cell structure and function. These include, but are not limited to, calpain activation (Lipton, 1999), lipid peroxidation (Braughler and Hall, 1992), nitric oxide synthesis (Bolanos et al., 1997) and mitochondrial free radical production (Camello-Almaraz et al., 2006). However, Ca^{2+} also plays a salient role in cell death, with excessive intracellular Ca^{2+} accumulation leading to over-activation of Ca^{2+} dependent pathways that are the final common mechanism for damage and/or death of a variety of CNS cell types (Tekkok and Goldberg, 2001; Prilloff et al., 2007). Following neurotrauma, neurons and glia close to the site of insult are vulnerable to secondary degeneration and may undergo delayed

death *via* a multitude of these Ca^{2+} dependent cellular and molecular cascades. Downstream mechanisms of damage include glutamate excitotoxicity (Doble, 1999; Hausmann, 2003; Matute et al., 2006), inflammation (Hausmann, 2003), Wallerian degeneration (Kerschensteiner et al., 2005; Weishaupt et al., 2010), glial scarring (Fawcett and Asher, 1999), dysmyelination (Totoiu and Keirstead, 2005; Payne et al., 2011), and apoptosis (Liu et al., 1997).

Ca^{2+} is known to enter neurons and glia through a range of channels and receptors, including but not limited to: voltage-gated Ca^{2+} channels (VGCCs) (Agrawal et al., 2000); purinergic $P2X_7$ receptors (Matute et al., 2007); glutamate-gated, GluR2 subunit lacking, Ca^{2+} permeable ionotropic α-amino-3-hydroxy-5-methyl-4-isoxazolepropionic acid receptors (AMPARs) (Hollmann et al., 1991); and *N*-methyl-D-aspartate receptors (NMDARs) (Matute, 2006). Increased glutamate is a common consequence following injury to the CNS (Doble, 1999) and can lead to over-activation of NMDA and AMPA receptors on neurons and glia, specifically oligodendrocytes, rendering these cells susceptible to increased Ca^{2+} influx and depolarisation (Matute et al., 1997; Doble, 1999). ATP also typically increases in response to injury (Neary et al., 2005), which can directly injure vulnerable cells, as well as trigger ATP-gated Ca^{2+} influx (Matute et al., 2007). Reactive species such as cell permeant H_2O_2 are generated as a consequence of injury both *in vivo* (Cornelius et al., 2013; O'Hare Doig et al., 2014a) and *in vitro* (Mandavilli et al., 2005; Ma et al., 2012), and also lead to increased influx through Ca^{2+} channels (Muralidharan et al., 2016). As such, over-activation of Ca^{2+} channels and receptors results in an appreciable influx of Ca^{2+} into cells. As a consequence of both Ca^{2+} and reactive species entry, mitochondria swell, oxidative metabolism is compromised, and cytochrome *c* is released into the cytoplasm, associated with oxidative damage to DNA, lipids and proteins, and neuronal and glial cell death (Gandhi et al., 2009; Huang et al., 2009; Kowaltowski et al., 2009a).

Given the consequences of excessive Ca^{2+} entry into neurons and glia following injury, the administration of Ca^{2+} channel inhibitors has been assessed as a therapeutic strategy for treatment of CNS damage *in vivo*. In rodent models of ischemia, application of nimodipine, an L-Type VGCC inhibitor, resulted in significant functional recovery (Ouardouz et al., 2003) and attenuated mitochondrial injury and apoptosis (Tanaka et al., 2004). However, nimodipine has also been found to cause hypotension and further ischemic injury to the spinal cord (Fehlings et al., 1989). Lomerizine (Lom), a dual L- and T-type VGCC inhibitor which

is currently in clinical use for the treatment of migraines, has been shown to act more specifically on the CNS with adverse systemic side effects avoided (Hara et al., 1999). We have demonstrated reduced retinal ganglion cell death and microglia/macrophage infiltration, preservation of myelin compaction and limited functional improvements following treatment of partial CNS injury with lomerizine (Fitzgerald et al., 2009), but clinical trials of lomerizine for treatment of neurotrauma are lacking.

A relatively limited number of $P2X_7R$ antagonists have been developed (Baraldi et al., 2000; Baraldi et al., 2002; Baraldi et al., 2003). One of the more effective of these is adenosine 5'-triphosphate periodate oxidized sodium salt (oxATP), an irreversible, non-competitive antagonist of $P2X_1$, $P2X_2$ and $P2X_7$ receptors, which has been shown to protect against secondary injury, and improve functional outcomes in rats following acute impact spinal cord injury (SCI) (Wang et al., 2004). NBQX, an AMPAR antagonist, has been shown to have neuroprotective effects following cerebral ischemia (Gill, 1994; Graham et al., 1996) and reduce excitotoxic insult in white matter following injury (Follett et al., 2000). However, NBQX has poor water solubility, and renal toxicity has limited use of this drug in the clinic (Xue et al., 1994). More recently, a highly selective novel competitive AMPA receptor antagonist [2,3-dioxo-7-(1*H*-imidazol-1-yl)6-nitro-1,2,3,4-tetrahydro-1-quinoxalinyl] acetic acid monohydrate (YM872 or "INQ"), with high solubility, was developed. YM872 has been assessed in a number of clinical trials of neuroprotection (Takahashi et al., 1998), however it was abandoned in phase-III human clinical trials for stroke in 2010, after failing an interim futility analysis (Klein and Engelhard, 2010). 3,5-dimethyl-1-adamantanamine (memantine or "Mem") is a non-competitive NMDAR antagonist, shown to provide neuroprotection with minimal side effects in animal models of ischemia (Block and Schwarz, 1996; Ehrlich et al., 1999). Memantine therapy has shown beneficial effects after brain injury, including alleviation of neurobehavioral deficits (Huang et al., 2015).

Whilst promising results have been demonstrated in pre-clinical studies, the translation of these therapeutic agents to the clinic has been limited and outcomes have been disappointing, highlighting the clear need for a new approach. Given the multiple routes of Ca^{2+} entry associated with the detrimental aspects of neurotrauma, it is becoming increasingly recognized that a combinatorial treatment strategy may be required (Tuszynski, 2005; Stack et al., 2006). We recently tested this hypothesis *in vivo*, assessing the efficacy of various combinations of three Ca^{2+} channel inhibitors at reducing secondary degeneration assessed 3 months following partial optic nerve transection in Piebald Viral Glaxo (PVG) rats (Savigni

et al., 2013). We used Lom to inhibit L- and T-type VGCCs, oxATP to inhibit $P2X_7Rs$, and/or YM872, to inhibit Ca^{2+} permeable AMPARs. Each of the treatment combinations involving lomerizine significantly increased the proportion of axons with normal compact myelin, implying a role for excess Ca^{2+} entry *via* VGCCs in myelin decompaction. In areas of nerve vulnerable to secondary degeneration, there is a significant increase in node of Ranvier length, associated with loss of visual function (Szymanski et al., 2013). Only administration of the three Ca^{2+} channel inhibitors in combination (Lom + oxATP + YM872) resulted in maintenance of normal node of Ranvier length(s), and preservation of function, with the remaining combinations proving less effective (Savigni et al., 2013).

However, an association between intracellular Ca^{2+} concentration and the viability of neurons and glia following treatment with combinations of Ca^{2+} channel inhibitors has not yet been established. Therefore here, the effects of combinations of the inhibitors (Lom, OxATP, YM872 and/or Mem) on excess Ca^{2+} influx and associated cell death of multiple cell types were determined, using a high throughput, *in vitro* model of oxidative injury in primary mixed cortical cultures (Whittemore et al., 1994). Note that the phrase "Ca^{2+} channel inhibitors" is used throughout, with the understanding that Ca^{2+} permeable AMPARs, $P2X_7Rs$ and NMDARs are also permeable to other ions that may be playing a role. Hydrogen peroxide (H_2O_2) was chosen as the reactive species stressor given its relative stability and established role in inducing oxidative damage in neurons and glia (Haskew-Layton et al., 2010).

Materials and Methods

Animals

PVG rat pups (postnatal days 0-3) were obtained from the Animal Resource Centre (Murdoch, Western Australia). All procedures were approved by The University of Western Australia Animal Ethics Committee (Ethics Approval Number RA3/100/673) and conformed to the National Health and Medical Research Council (NHMRC) of Australia Code of Practice for use of Animals for Scientific Purposes. All efforts were made to minimise animal suffering and to reduce the number of animals used. Rat pups were euthanized with intraperitoneal injection of Lethabarb© (Pentobarbital sodium 850mg/kg, Virbac). For each

cell culture preparation, cortices from two to six animals were pooled together, depending upon cell numbers required. 85 animals were used in the experiments of the study.

Tissue dissection

Following euthanasia, the skin overlying the skull was removed, and the skull was peeled away. Deep cuts were made at the margin of the cortex and superior colliculi caudally (both sides) and again at the border of the olfactory lobes, and cortex rostrally. The middle section of the brain with cortices intact was removed from the skull, and transferred to a sterile petri dish containing cold (~4˚C) Neurobasal®-A medium (NB-A, Life Technologies). The cortex was then peeled away from underlying midbrain structures and the meninges were teased off. The 'naked' cortex was then transferred to a second sterile petri dish containing cold NB-A. Once all tissue was collected, a scalpel blade was used to chop the cortices into small pieces, which were transferred using a transfer pipette to a 50mL falcon tube containing 10mL NB-A.

Cell culture

Mixed cortical (MC) cells were prepared as described in (Whittemore et al., 1994). In brief: following an initial 3 minute (min), 200g centrifugation, tissue was enzymatically digested in 10mL Phosphate Buffered Saline (PBS; Invitrogen) solution containing 165U papain (Worthington), 3000U of DNase 1 from bovine pancreas (dissolved in Earls Balanced Salt Solution; both from Sigma-Aldrich), 1.65µM cysteine (Sigma-Aldrich) and 50µM NaOH for 5 minutes (min), at 37˚C. Enzyme treated tissue pieces were centrifuged for 22 min at 200g, enzyme solution was removed and tissue was dissociated in 10mL of NB2 media, consisting of: Neurobasal®-A medium (NB-A), containing 500µM glutamine (Life Technologies), 2% B27 (Life Technologies), 100U/mL penicillin (Invitrogen) and 100µg/mL streptomycin; (Invitrogen). All multi-well plates and coverslips were pre-coated with poly-L-lysine (10µg/mL) in UltraPure™ distilled water, for one hour (h) at room temperature, followed by washing 3x with PBS prior to cell seeding. MC cells were seeded at $1.5x10^5$ cells/cm^2 in NB2: into 12 well plates containing 15mm coverslips (for calcium imaging); or 24 well plates (for live/dead viability assay). Following seeding, cells were allowed to incubate for 24 h after which NB2 media was replaced with fresh media containing 57% NB2 and 43% NB1 media (NB2/NB1 growth media). NB1 media is NB2 media supplemented with 4.2% fetal calf serum (Life Technologies), 1% (v/v) horse serum (Life Technologies), 26.7µM L-

glutamic acid monosodium salt hydrate (Sigma-Aldrich), and 22.2µM 2-mercapathoethanol (Life Technologies). NB2/NB1 media was replaced every 48-72 h.

Treatments

Effects of combinations of Ca^{2+} channel inhibitors, Lom (LKT Labs), OxATP (Sigma), YM872 (LKT Labs), and/or Mem (Sigma) were assessed. Choices of treatment concentrations were based on previously published studies using these agents individually. Lom was dissolved in dimethyl sulfoxide (DMSO) before being added to medium at a final concentration of 1µM (Tamaki et al., 2003): final concentration of DMSO was less than 1% v/v. OxATP (1mM; (Matute et al., 2007)), YM872 (240µM; (Savigni et al., 2013)) and Mem (60µM, (McAllister et al., 2008)) were dissolved in medium. Ca^{2+} channel inhibitors were administered to cultures such that all possible combinations of single and multiple inhibitors were assessed.

Analysis of inhibitor and H_2O_2 stability

Stability of the inhibitors in the presence and absence of H_2O_2 were assessed by reverse phase High Performance Liquid Chromatography (HPLC), on a Waters 2695 HPLC with a Waters 2489 UV/vis detector with elution through a C18 analytical column (150 x 4.60 mm, 5 µm, 25°C). For all inhibitors, the ratio of inhibitor:H_2O_2 concentration equated to those used in cell analysis experiments, described below. For OxATP, two samples were prepared by dissolving OxATP in water in the absence and presence of H_2O_2 (OxATP:H_2O_2, 1:0.4). A mobile phase of Acetonitrile (A):0.1M Phosphate buffer pH 7 (B) was used with gradient elution and varying flow rates as follows: 0 mins, 100% B at 0.85ml/min; 4 mins, 95% B at 0.8 ml/min; 8 mins, 75% B at 1mL/min; 12 mins, 70% B at 1 ml/min. Injection volume was 10µL, detection wavelength was 254nm with retention times of 5.4 min (OxATP) and 5.2 min (OxATP + H_2O_2). Total run time was 12 mins.

For Lomerizine and YM872 the mobile phase consisted of Water with 0.5% Trifluoroacetic acid:Acetonitrile (31:69 v/v) with isocratic elution at 0.5ml/min. Total run time was 15 mins, detection wavelength was 210nm and sample injection volume was 1µL. Lomerizine was dissolved in methanol in the absence and presence of H_2O_2 (Lom:H_2O_2, 1:400) with retention times of 4.7 mins. However, an additional peak at 3.3 min was evident in the presence of H_2O_2 indicating possible degradation of lomerizine. YM872 was dissolved in water in the absence and presence of H_2O_2 (YM872:H_2O_2, 1:1.65) with retention times of 2.9 mins.

Stability of H_2O_2 in the presence and absence of the compounds was measured by fluorescence detection of H_2O_2 using the hemin-catalyzed oxidation of p-hydroxyphenylacetic acid to yield the fluorescent dimer. Briefly, p-hydroxyphenylacetic acid (80μM) and hemin (8μM) were dissolved in ammonia buffer, pH 10. This solution was then used to prepare samples of H_2O_2 (400μM) in the absence and presence of: YM872, OxATP, Lomerizine (see compound:H_2O_2 ratios detailed above) and Memantine (Memantine:H_2O_2, 1:6.7). Fluorescence was measured in triplicate on a Varian Cary Eclipse instrument with excitation at 320nm and emission at 410nm in a 1mL cuvette with a 10mm path length. Average fluorescence intensity was 40 ± 0.5 in the absence and presence of each of the compounds.

Cell analysis

The following experiments were undertaken following 10 days of culture in NB2/NB1growth media at 37˚C (95% air/5% CO_2 v/v). Control cultures were incubated in identical fashion but without H_2O_2, and/ or without the addition of Ca^{2+} channel inhibitors or other modulators as detailed below.

Live Ca^{2+} imaging: Ca^{2+} imaging was performed on MC cells attached to glass coverslips at room temperature, using the ratiometric Ca^{2+} sensitive dye Fura-2AM (Invitrogen). All solutions were prepared immediately prior to imaging. Cells were loaded with 4μM Fura-2AM in NB-A (+10mM HEPES, without phenol red; Life Technologies) at room temperature, for 30 min, then gently washed with Hanks Balanced Salt Solution (HBSS; Life Technologies). Coverslips were then transferred to an RC-26G chamber system (Warner Instruments) containing 1mL NB-A (+10mM HEPES). Images were captured every 15 seconds for 2 min in order to measure basal Ca^{2+} levels. A pre-prepared solution containing a final H_2O_2 concentration of 400μM ± Ca^{2+} channel inhibitors (at concentrations described above), and/ or the ryanodine receptor agonist ryanodine (20μM, 40μM, or 60μM; Sigma-Aldrich) or the Zn chelator N,N,N',N'-Tetrakis(2-pyridylmethyl)ethylenediamine (TPEN, 1 or 10μM; Sigma-Aldrich) was then applied to the chamber at the beginning of a 30 min acquisition. The choice of H_2O_2 concentration was based upon previous studies and our own pilot experiments that indicated 400μM provides a sustained and consistent increase in intracellular Ca^{2+} without biphasic effects or oscillations (Herson et al., 1999). In initial experiments, individual intracellular Ca^{2+} concentrations were determined. MC cells were incubated with Fura-2 AM as above and imaged for 10min following addition of 10μM

ionomycin (Molecular Probes) in HBSS (+3mM Ca^{2+}, Mg^{2+}) to determine R_{max} values. MC cells were then washed gently with HBSS (Ca^{2+} free) and imaged for another 10 min following addition of 10μM BAPTA AM (Molecular Probes). The mean intracellular Ca^{2+} concentration at baseline (no H_2O_2 present) was ~73nM.

Cells were visualized using an Olympus BX51WI upright microscope equipped with an XM10 monochrome CCS camera (Olympus). Imaging was performed at x60 magnification, capturing a field of view of 147.2μm x 100.4μm, with an exposure time of 20ms and 2x2 pixel binning. Regions of interest (ROIs) per field of view (FOV) were defined for each individual cell within the FOV, and were used to determine F340/F380 ratios using Olympus Xcellence RT software. One FOV per coverslip was assessed, consistent for all coverslips.

Cell viability: MC cells were incubated in H_2O_2 ± Ca^{2+} channel inhibitors and/or Ethylene glycol-bis(2-aminoethylether)-*N,N,N',N'*-tetraacetic acid (EGTA; 10μM, 0.1mM or 1mM; Sigma-Aldrich) for 30 min, 6 or 24 h. Immediately following the incubation, cells were gently rinsed with HBSS, and incubated with 1μM Calcein-AM (Invitrogen) and 2μM Ethidium homodimer (Ethd-1; Invitrogen) for 30 min. Cultures were then imaged at x40 magnification using an Olympus IX51 inverted fluorescence microscope. FOV were randomly assigned and consistent for all culture wells. Viability was quantified by counting all viable and dead cells in 2 FOV per well (450μm x 350μm), with three wells per condition. Data were expressed as the percentage of viable cells ± S.E.M.

Densities of individual cell populations: MC cells were incubated in H_2O_2 ± Ca^{2+} channel inhibitors for 30 min, 6 or 24 h. Following incubation, cell cultures were washed 3x with PBS, then fixed with 2% v/v paraformaldehyde (PFA; 0.1M phosphate buffer; pH 7.2) for 10 min, followed by a further 20 min with 4% v/v PFA (0.1M phosphate buffer; pH 7.2). Cells were then washed a further 3x with PBS and immunohistochemical analyses conducted according to established procedures (Fitzgerald et al., 2010a), using primary antibodies to identify specific cell types: neurons, β-III tubulin (1:1000; Covance); astrocytes, glial fibrillary acidic protein (GFAP; 1:500; Sigma-Aldrich); NG2+ non-oligodendroglial cells, NG2+ (1:500; Abcam) / Olig2- (1:500, R and D Systems); oligodendroglia, Olig2; activated microglia/ macrophages (ED1; 1:500; Abcam) and Hoechst nuclear stain (1:2000; Invitrogen). Secondary antibodies were species specific AlexaFluor® 488 and 555 (1:400; Invitrogen). Cultures were imaged at x40 magnification using an Olympus IX51 inverted fluorescence microscope. Quantification of densities of individual cell populations was

conducted by counting all immunopositive cells in 4 FOV per well (450µm x 350µm), with 2 wells/treatment group. FOV were randomly assigned and consistent for all culture wells. Mean number of immunopositive cells were expressed per mm^2.

Statistical analyses

All statistical analyses were performed using SPSS® Version 20 (IBM©) analysis software. For analysis of live cell calcium imaging, all data were derived from 3-5 independent experiments, each experiment using cells prepared from separate groups of rat pups. Variability between experiments was examined and we did not find outliers from specific experiments. Because of the large number of inhibitor combinations being compared it was not feasible to conduct all assessments within each single experiment. Therefore, in accordance with best practice in the published literature (Zhang et al., 2005), data from the experiments were combined for the final statistical analyses. A minimum of 14 and frequently as many as 40 cells in total were assessed for each treatment condition. The baseline F340/F380 ratios were averaged and at each time point, F340/F380 ratios were divided by the mean baseline (F340/F380 ratio before addition of H_2O_2 +/- inhibitors) to give a ΔF-Ratio. As experiments were conducted on mixed cultures it was not appropriate to convert ΔF-Ratios to Ca^{2+} concentrations, due to established variabilities between Ca^{2+} concentrations in neurons and glia (Suadicani et al., 2010) and altered responses to stressors (van den Pol et al., 1992). ΔF-Ratios were compared using two-way repeated measures analysis of variance (ANOVA), with Games-Howell post-hoc tests ($\alpha = 0.05$) to compare $H_2O_2 \pm Ca^{2+}$ channel inhibitors to H_2O_2 treated cultures, at each time point assessed during the 30 min incubation period. Analyses of cellular viability were conducted using a two-way ANOVA ($\alpha = 0.05$), with Games-Howell post-hoc tests to compare $H_2O_2 \pm Ca^{2+}$ channel inhibitors to H_2O_2 control at each time point. Analyses of densities of individual cell types were conducted using a two-way ANOVA ($\alpha = 0.05$), with Dunnett's post-hoc tests to compare $H_2O_2 \pm Ca^{2+}$ channel inhibitors to H_2O_2 control at each time point. All data were expressed as means ± standard error of the mean (S.E.M.); F and degrees of freedom (df) are reported for each ANOVA conducted and subsequent p values refer to *post hoc* test outcomes.

Results

Differential reduction in intracellular Ca^{2+} with various Ca^{2+} channel inhibitor combinations

H_2O_2 insult resulted in gradual increases in mean ΔF-Ratio (indicative of changes in intracellular Ca^{2+} concentration) in MC cells over a 30 min incubation period, relative to control (Fig. 1B), with a significant increase demonstrated at 30 min ($df = 1$, $F = 15.67$, $p \leq 0.05$; representative images Fig. 1A). The intracellular Ca^{2+} concentration of MC cells not exposed to H_2O_2 did not change ($p > 0.05$, Fig. 1A, B). Increases in intracellular Ca^{2+} concentration can occur *via* influx across the cell membrane (extracellular source) or release from intracellular Ca^{2+} stores. The contribution of ryanodine receptor dependent release of Ca^{2+} from the endoplasmic reticulum was assessed by challenging the cultures with increasing concentrations of the antagonist ryanodine simultaneously with H_2O_2 insult. 40μM ryanodine was required to reduce the ΔF-Ratio at 30 min relative to H_2O_2 control ($df = 4$, $F = 32.27$, $p \leq 0.05$, Fig. 1B). However, the ΔF-Ratio in the presence of 40μM ryanodine remained higher than in controls without H_2O_2 at this time ($p \leq 0.05$, Fig. 1B), indicating additional sources of intracellular Ca^{2+}. Additional control experiments were conducted to assess the effect of ryanodine alone as well as the potential contribution of Zn to the Fura-2 signal, given that under some conditions Fura-2 can detect free Zn (Grynkiewicz et al., 1985). Addition of Ryanodine alone at the tested concentrations did not stimulate Ca^{2+} release above control levels at 30 min ($df = 4$, $F = 13.83$, $p > 0.05$, Fig. 1B). Addition of the Zn chelator TPEN to cultures simultaneously with H_2O_2 insult also did not significantly reduce the ΔF-Ratio at 30 min, relative to H_2O_2 alone ($p > 0.05$, Fig. 1C), indeed there was a non-significant trend to an increase with the chelator, indicating that the ΔF-Ratio was not increased due to contributions from free Zn.

In the absence of cells, HPLC stability analyses of Lom, oxATP and YM872 incubated for 30 min in the presence of H_2O_2, demonstrated that there was no effect of H_2O_2 on oxATP or YM872 stability, but lomerizine was degraded by approximately 15% (data not shown). Memantine could not be analysed due to the lack of a chromophore that could be detected by HPLC. Additionally, fluorescence detection of H_2O_2 indicated that H_2O_2 stability did not alter in the presence of each of the inhibitors, confirming a lack of a direct effect of the inhibitors on H_2O_2 and indicating that outcomes to be measured were due to effects of the inhibitors on cells.

The effects of all possible combinations of the Ca^{2+} channel inhibitors Lom, oxATP, YM872, and/or Mem on the intracellular Ca^{2+} concentration (ΔF-Ratio) of H_2O_2 stressed MC cells were assessed. The changes in Ca^{2+} concentration are expressed relative to the baseline Ca^{2+} concentration in the same culture before the addition of H_2O_2 and inhibitors. Ca^{2+} channel inhibitors were administered to cultures singly, in pairs, in groups of three or all four inhibitors, and ΔF-Ratios were compared to outcomes from H_2O_2 treated cultures without inhibitors. Of the single inhibitors, only oxATP significantly reduced ΔF-Ratio at 30 min ($df = 16$, $F = 20.78$; $p \leq 0.05$, Fig. 2A, Fig. 2B). Of the combinations of two inhibitors, only Lom + YM872, Lom + Mem, oxATP + YM872, and oxATP + Mem significantly reduced ΔF-Ratio ($df = 16$, $F = 20.78$, $p \leq 0.05$; Fig. 2A, Fig. 2C). The trend to an increased ΔF-Ratio with Mem + YM872 was not significant at any time point ($p > 0.05$). The finding that Lom + YM872 resulted in a significant reduction in ΔF-Ratio whereas YM872 alone did not, confirmed that the concentration of lomerizine used was sufficient to cause a biological effect despite some degradation in the presence of H_2O_2. Of the remaining combinations of three or four inhibitors, only Lom + oxATP + YM872, oxATP + YM872 + Mem, and Lom + oxATP + YM872 + Mem significantly reduced ΔF-Ratio ($df = 16$, $F = 20.78$, $p \leq 0.05$; Fig 2A, Fig. 2D). It is important to note that the apparently higher ΔF-Ratio following treatment with Lom + oxATP + Mem was not significantly different to the H_2O_2 control. This trend towards an anomalous finding was likely due to differences in ROI numbers between the two groups and the somewhat high variability observed with this inhibitor combination. Comparisons between ΔF-Ratios from MC cells treated with the various inhibitor combinations that reduced intracellular Ca^{2+} concentration relative to H_2O_2 without inhibitors, did not reveal significant differences between these inhibitor combinations at 30 min ($p > 0.05$, Fig 2A).

Differential reduction in cell viability with various Ca^{2+} channel inhibitor combinations

The association of acute changes in Ca^{2+} concentration with cell viability at 30 minutes as well as at later time points (i.e. 6, 24 h), was assessed in MC cells exposed to H_2O_2 insult. Following 30 min incubation with H_2O_2, the time point at which Ca^{2+} imaging was performed, there was no significant decrease in the percentage of viable cells relative to control (Fig. 3A, B). At 6 h, the percentage of live cells was significantly reduced, and remained significantly reduced at 24 h ($p \leq 0.05$, Fig. 3A, B) relative to control. The density of cells in control cultures was 1001.36 ± 70.18 cells/mm^2, was not significantly reduced at 30 min (1129.36 ± 84.92 cells/mm^2) but was significantly reduced at 6 (379.36 ± 54.51

cells/mm^2) and 24 h (405.08 ± 117.72 cells/mm^2, $p \leq 0.05$) relative to control (731.75 ± 93.75 and 658.73 ± 48.66 cells/mm^2 respectively).

The effects of Ca^{2+} channel inhibitor combinations on cell viability were assessed at 6 h; the choice of 6 h as opposed to 24 h was based upon the aim of assessing changes in viability associated with altered Ca^{2+} concentrations at 30 min, while minimising secondary effects likely to contribute to cell death at later time points. Of the fifteen Ca^{2+} channel inhibitor combinations, only seven combinations significantly increased the percentage of live cells compared to H_2O_2 control ($df = 16$, $F = 29.36$, $p \leq 0.05$). Specifically, of the single inhibitors, only oxATP significantly increased the percentage of viable cells ($p \leq 0.05$, Fig. 4). Note that reductions in intracellular Ca^{2+} concentration with single inhibitors (Fig. 2A, B) were directly associated with improvements in cell viability. Of the combinations of two inhibitors, only Lom + oxATP, oxATP + YM872, and oxATP + Mem significantly increased the percentage of live cells compared to H_2O_2 control ($p \leq 0.05$, Fig. 4). It is interesting to note that improvements in cell viability with treatment with Lom + oxATP were not associated with reduced intracellular Ca^{2+} concentration, whereas treatment with oxATP + YM872 and oxATP + Mem were associated both with reduced intracellular Ca^{2+} concentration (Fig. 2A, B) and improved viability. In contrast, Lom + YM872 and Lom + Mem treatments, which were observed to decrease intracellular Ca^{2+} concentration (Fig. 2A, B), had no effect on cell viability ($p > 0.05$, Fig. 4). Of the remaining combinations of three or four inhibitors, Lom + oxATP + YM872, Lom + oxATP + Mem, oxATP + YM872 + Mem, as well as Lom + oxATP + YM872 + Mem all significantly increased the percentage of viable cells ($p \leq 0.05$, Fig. 4). These improvements in cellular viability were directly associated with reductions in intracellular Ca^{2+} concentration for Lom + oxATP + YM872, oxATP + YM872 + Mem, and Lom + oxATP + YM872 + Mem treatments (Fig. 2A, B). However Lom + oxATP + Mem improved viability without altering intracellular Ca^{2+} concentration (Fig. 2A, 4). The effects of oxATP on viability in decreased extracellular Ca^{2+} concentrations were assessed using increasing concentrations of EGTA to chelate Ca^{2+}. The chosen EGTA concentrations have been shown to decrease extracellular Ca^{2+} concentration while maintaining cell viability (Takadera et al., 2010). EGTA alone had no significant effect on cell viability, and viability was significantly higher than H_2O_2 control at each of the tested concentrations ($df = 11$, $F = 23.90$; $p \leq 0.05$, Fig. 5). In the presence of H_2O_2, 1mM EGTA significantly increased cell viability compared to H_2O_2 control, indicating that increased extracellular Ca^{2+} contributes to H_2O_2 insult; lower EGTA concentrations had no significant effect. In contrast, in the presence

of oxATP, all tested concentrations of EGTA significantly increased cell viability compared to H_2O_2 control ($p \leq 0.05$, Fig. 5), which together with the demonstrated reduction of intracellular Ca^{2+} with oxATP (Fig. 2A), implies that the protective role of oxATP is Ca^{2+} dependent.

Increased viability of neurons, astrocytes, and NG2+ non-oligodendroglial cells with various Ca^{2+} channel inhibitor combinations

Early reductions in intracellular Ca^{2+} concentration were not always associated with improvements in cell viability at 6 h. It was therefore postulated that the Ca^{2+} channel inhibitor combinations may have differential effects on viabilities of specific cell sub-populations within the MC cultures. Accordingly, a selection of Ca^{2+} channel inhibitor combinations with a range of effects was used, and densities of individual cell sub-populations assessed. The Ca^{2+} channel inhibitor combinations tested were oxATP, Lom + oxATP, Lom + oxATP + Mem, Lom + oxATP + YM872, and Lom + oxATP + YM872 + Mem. Cell sub-populations were: β-III tubulin+ cells that are predominantly neurons (Katsetos et al., 1993); astrocytes (GFAP+); NG2+ non-oligodendroglial cells, likely to be predominantly pericytes and in some circumstances macrophages (Dimou and Gallo, 2015) (NG2+/Olig2-); oligodendroglia (Olig2+); and activated microglia/ macrophages (ED1+). The Olig2+ sub-population comprised approximately 70% Olig2+/NG2+ oligodendrocyte precursor cells; the remainder were Olig2+/NG2- and were therefore likely to be more mature oligodendrocytes. Following H_2O_2 insult in the absence of inhibitors, there was a statistically significant reduction in the density of β-III tubulin+, GFAP+, NG2+/Olig2-, Olig2+ and ED1+ cells, compared to control ($df = 7$, $F = 14.38, 4.82, 9.06, 22.95$, respectively, $p \leq 0.05$, Fig. 6). In the presence of the six Ca^{2+} channel inhibitor combinations and H_2O_2, treatment with the five combinations that included oxATP resulted in significantly increased density of at least one of the cell sub-populations compared to the H_2O_2 only control ($p \leq 0.05$, Fig. 6). However, no one inhibitor combination was uniformly effective. Specifically, H_2O_2 stressed cultures treated with Lom + oxATP + YM872 or Lom + oxATP + YM872 + Mem significantly increased the density of β-III tubulin+ cells ($p \leq 0.05$, Fig. 6A, B). However, while the increases were significant, the degree of improvement was minor (Fig. 6A). Only treatment with Lom + oxATP + YM872 + Mem resulted in significantly increased density of GFAP+ cells ($p \leq 0.05$, Fig. 6C), with densities following all remaining treatments not significantly different from H_2O_2 only control ($p > 0.05$, Fig. 6C, D). Treatment with oxATP, Lom + oxATP, Lom + oxATP + YM872, and Lom + oxATP + Mem significantly increased

the density of NG2+/Olig2- cells compared to H_2O_2 only control ($p \leq 0.05$, Fig. 6E). However, only treatment with Lom + oxATP + YM872 and Lom + oxATP + Mem resulted in preservation of these NG2+/Olig2- cells to densities not significantly different to control ($p > 0.05$, Fig. 6E, F). No combinations of Ca^{2+} channel inhibitors were observed to have a significant effect on density of Olig2+ oligodendroglia or ED1+ microglia/ macrophages, compared to H_2O_2 only control ($p > 0.05$; Fig 6 G-J).

Discussion

Using a high throughput *in vitro* model of CNS injury and multiple combinations of four Ca^{2+} channel inhibitors, we demonstrate that intracellular Ca^{2+} concentration is not always directly related to cell viability. Furthermore, while individual cell sub-populations were vulnerable to H_2O_2 insult, only some sub-populations could be rescued by treatment with Ca^{2+} channel inhibitors. Specifically, most Ca^{2+} channel inhibitor combinations including oxATP preserved NG2+ non-oligodendroglial cells, but preservation of astrocytes and neurons required additional inhibitors. $Olig2^{+}$ oligodendroglia and $ED\text{-}1^{+}$ activated microglia/ macrophages were not preserved by any of the inhibitor combinations.

Intracellular Ca^{2+} has been shown to be sequestered into mitochondria during excitotoxicity, triggering mitochondrial dysfunction and oxidative stress (Dykens, 1994; Lau and Tymianski, 2010). Reactive oxygen species (ROS) are generated as natural by-products of oxidative metabolism, and are vital for cell signaling and homeostasis (Kowaltowski et al., 2009b). However, exposure of mitochondria to increasing Ca^{2+} influx results in a secondary feed-forward mechanism whereby ROS production is enhanced (Dykens, 1994). This phenomenon has now been demonstrated for many cell types including neurons (Kahlert et al., 2005), cardiac myocytes (Viola et al., 2007) and vascular smooth muscle (Chaplin et al., 2015). Excess ROS can spread, leading to oxidative damage *in vivo* (Kowaltowski et al., 2009b; Fitzgerald et al., 2010b). Following injury to the central nervous system, infiltrating inflammatory cells that enter the injury site are a significant additional source of ROS, including H_2O_2 (O'Hare Doig et al., 2014b). Multiple feed forward mechanisms that result in ROS initiate further increases in intracellular Ca^{2+} levels, contributing to additional cell death (Kristian and Siesjo, 1998). Proposed mechanisms by which H_2O_2 causes increased intracellular Ca^{2+} levels include activation of VGCCs (Roveri et al., 1992), nonspecific changes in membrane permeability to Ca^{2+} (Rojanasakul et al., 1993), changes in the Na^{+}-Ca^{2+} exchanger (Kaneko et al., 1989), and H_2O_2 induced Ca^{2+} release from intracellular stores (Nicotera and Rossi, 1994). Our data indicate that both release of Ca^{2+} from ryanodine sensitive intracellular stores and influx of extracellular Ca^{2+} through $P2X_7R$ as well as other Ca^{2+} channels contribute to the rise in intracellular Ca^{2+} levels following H_2O_2 insult.

Given the consequences of excessive Ca^{2+} entry into neurons and glia following injury, it was hypothesized that reductions in intracellular Ca^{2+} levels following treatment with Ca^{2+} channel inhibitors would be associated with increased cell viability. Reductions in

intracellular Ca^{2+} concentration with oxATP treatment were directly associated with substantial improvements in cell viability. However, treatment with the inhibitor combinations Lom + oxATP, Lom + YM872 and Lom + Mem revealed that dissociation between intracellular Ca^{2+} concentration and cell viability can occur in this model system. Thus, one cannot simply assume that intracellular Ca^{2+} overload results in cell death. As cell viability was increased following treatment with all combinations of inhibitors that included oxATP, the results indicate that controlling intracellular Ca^{2+} concentration by limiting influx *via* P_2X_7Rs may play an important role in maintaining cortical cell viability *in vitro* following insult. As such, the data support the '*source specificity hypothesis*' whereby Ca^{2+} cytotoxicity is not merely a function of increased Ca^{2+} concentration, but instead is linked to specific second messenger pathways activated by excessive Ca^{2+} entry through specific channels (Tymianski et al., 1993). Interestingly however, treatment with Lom + YM872 or Lom + Mem were not protective, and nor were YM872 or Mem alone. Furthermore, almost all combinations of Ca^{2+} channel inhibitors that included both YM872 + Mem were not protective: exceptions were treatments that included oxATP. While somewhat speculative at this stage, it is possible that Ca^{2+} influx through both Ca^{2+} permeable AMPAR and/ or NMDAR is necessary for MC cell health following H_2O_2 insult, and that the cytotoxic consequences of excessive Ca^{2+} through these channels can be overcome by the inhibitory action of oxATP on P_2X_7Rs and subsequent downstream events. Inhibition of flux of other ions through Ca^{2+} permeable AMPAR, P_2X_7Rs and NMDAR may also influence viability.

The apparent dissociation between intracellular Ca^{2+} concentration and MC cell viability may have been due to masking of differential effects on individual cell sub-populations by the effects on the mixed cell population as a whole. Ca^{2+} imaging studies on pure neuronal and/or astrocyte cultures exposed to H_2O_2 stress and the multiple combinations of Ca^{2+} channel inhibitors were considered, however such studies would ignore the complexities of inter-cellular interactions, cytokine release in response to stress and inter-cellular transfer of reactive species via gap junctions. Increase in intracellular Ca^{2+} concentration in neurons *via* P_2X_7R ion channels plays a major role in mitochondrial dysfunction leading to apoptotic neuronal death (Nishida et al., 2012). However, treatment with oxATP was insufficient to protect neuronal density. Reports have indicated that neurons are particularly sensitive to H_2O_2 (Behl et al., 1994; Whittemore et al., 1994). Thus, it is likely that the 6 h H_2O_2 insult overwhelmed the protective effect of oxATP and additional inhibitors were required for even minimal neuroprotection. While there was a trend to protection of astrocytes by most of the

tested combinations of Ca^{2+} channel inhibitors, only the combination of all four inhibitors resulted in significant protection. Astrocytes release glutamate and ATP in the injured scenario *via* a number of mechanisms (Bal-Price et al., 2002; Ye et al., 2003) including $P2X_7Rs$ (Duan et al., 2003) and this can have detrimental effects on adjacent cells. The loss of astrocytes despite treatment with most inhibitor combinations may have limited their contribution to damage to surrounding cell sub-populations. NG2-glia are an abundant population of cells in the adult CNS that can generate multiple cell types including oligodendrocytes, type 2-astrocytes and pericytes (Richardson et al., 2011). NG2-glia have been shown to evoke increased intracellular Ca^{2+} concentrations in optic nerves *in situ* following $P2X_7R$ and AMPAR activation, with ATP alone evoking robust changes in intracellular Ca^{2+} (Hamilton et al., 2010). In the current study, inhibition of $P2X_7R$ with oxATP resulted in increased NG2-glia viability. However, protection was only observed for NG2+ cells that were not of an oligodendroglial lineage. Olig2+ oligodendroglia, were approximately 70% oligodendrocyte precursor cells, and not protected by any of the Ca^{2+} inhibitor combinations, likely reflecting the known selective vulnerability of OPCs to oxidative stress (Back et al., 1998). Despite a lack of protection of oligodendroglia by the tested inhibitor combinations *in vitro,* Lom treatment has been shown to preserve myelin compaction in vulnerable white matter following partial optic nerve transection *in vivo,* and short term delivery of oxATP + YM872 together with sustained delivery of Lom preserved node/paranode structure as well as visual function in this *in vivo* model (Savigni et al., 2013). These data indicate that the three Ca^{2+} channel inhibitors in combination have a beneficial effect on oligodendroglia *in vivo*. While the MC cells utilized in the current study contain many of the cell types found *in vivo,* three dimensional architecture and cellular interactions are lacking. It is increasingly understood that NG2-glia are required at the Node of Ranvier for axonal and myelin integrity (Butt et al., 1999). Our demonstration of protection of NG2+/olig2- cells by combinations of ion channels containing oxATP indicate that protection of these particular cells may be a critical element preserving structure and function of intact but vulnerable myelinated axons of the CNS *in vivo*.

Conclusions

The contribution of specific Ca^{2+} channels to excess Ca^{2+} influx in individual cell sub-populations in this *in vitro* model may not reflect the complexities of the injured CNS. Nevertheless, the data provide insight into effects of inhibition of individual and multiple

Ca^{2+} channels on cell sub-populations, with a breadth and scope not feasible in *in vivo* studies. The demonstration of protection of MC viability with oxATP alone and in combination with other Ca^{2+} channel inhibitors provides support for further *in vivo* investigation where the presence of oxATP is maintained long term after CNS injury.

Acknowledgements

We acknowledge financial support from the Neurotrauma Research Program of Western Australia, an initiative of the Road Safety Council of Western Australia. This project is funded through the Road Trauma Trust Account, Western Australia, but does not reflect views or recommendations of the Road Safety Council. We thank Dr Robert Gasperini for his helpful advice on Ca^{2+} imaging. MF is supported by an NHMRC Career Development Fellowship (APP1087114).

Figure Legends

Figure 1. Hydrogen peroxide insult increases intracellular Ca^{2+} in MC cells via intracellular and extracellular sources. Representative images show increased Fura340 fluorescence (blue) at 30 min in MC cells stressed with H_2O_2 (A); scale bar = 20µm. Quantification of ΔF-Ratio through analysis of Fura-2 AM emissions under 340/380 nm excitation, immediately preceding and following 400µm H_2O_2 insult, traces of mean data over time are shown (B): 3-4 separate experiments were conducted for each data point, encompassing a total of 27-40 cells/ treatment group. MC cells treated with H_2O_2 ± ryanodine (10µm, 20µm or 40µm) for 30 min, traces of mean data shown (B): 3-4 separate experiments encompassing a total of 10-20 cells/ treatment group. ΔF-Ratio in MC cells treated with H_2O_2 ± TPEN (1µm or 10µm) for 30 min, traces of mean data shown (D): 3-4 separate experiments were conducted, encompassing a total of 10-20 cells/ treatment group; note that the colouring of traces for control and H_2O_2 are represented using the same colours as in B.

Figure 2. Various combinations of Ca^{2+} channel inhibitors reduce the intracellular Ca^{2+} concentration of MC cells following H_2O_2 insult. ΔF-Ratios derived from Fura-2 AM emissions under 340/380 nm excitation immediately preceding and following 400µm H_2O_2 insult ± Ca^{2+} channel inhibitors at 30 min (A): 4-5 separate experiments were conducted, encompassing a total of 14-40 cells/ treatment group; * statistically significantly different from H_2O_2, $p \leq 0.05$. Note that while all control values at 0 min approach 1.0, they are not identical. Traces of mean ΔF-Ratios throughout the 30 min incubation period are shown for MC cells treated with single inhibitors (B), pairs of inhibitors (C) or three or 4 inhibitors in combination (D); note that the colouring of traces for control and H_2O_2 in C and D are represented using the same colours as in B.

Figure 3. Time dependent changes in MC cell viability with H_2O_2 insult. Mean ± SEM percent viable MC cells following incubation with 400µm H_2O_2 for 30 min, 6 or 24 h compared to control at each time point (A): * statistically significantly different from control at each time point, $p \leq 0.05$. Representative images of MC cells stained with Calcein-AM and Ethidium homodimer following incubation with 400µm H_2O_2 are shown (B), scale bar = 75µm.

Figure 4. Treatment with various combinations of Ca^{2+} channel inhibitors increases viability of MC cells following H_2O_2 insult. Mean ± SEM percent viable MC cells following incubation with 400μm H_2O_2 ± combinations of Ca^{2+} channel inhibitors for 6 h; * statistically significantly different from H_2O_2 only control, $p \leq 0.05$.

Figure 5. Effects of the Ca^{2+}chelator EGTA on MC viability in the presence of oxATP and H_2O_2 insult. Mean ± SEM percent viable MC cells following incubation with 400μm H_2O_2 ± oxATP, with or without increasing concentrations of EGTA for 6 h; * statistically significantly different from H_2O_2 only control, $p \leq 0.05$.

Figure 6. Treatment with various combinations of Ca^{2+} channel inhibitors increases viability of specific cell sub-populations. Mean ± SEM density (/mm^2) of βIII tubulin+ neurons (A), GFAP+ astrocytes (C), NG2+/Olig2- NG2+ non-oligodendroglial cells (E), Olig2+ oligodendroglia (G), and ED1+ activated microglia/macrophages (I) following incubation with 400μm H_2O_2 ± Ca^{2+} channel inhibitors for 6 h compared to control; * statistically significantly different from H_2O_2 only control, $p \leq 0.05$. Representative images of βIII tubulin+ neurons (green) (B), GFAP+ astrocytes (red) (D), NG2+ (green) /olig2- non oligodendroglial cells (F), Olig2+ (red) oligodendroglia (H) and ED1+ microglia/ macrophages (green) (J) are shown; all with Hoechst nuclear stain, scale bar = 100μm.

References

Agrawal SK, Nashmi R, Fehlings MG (2000) Role of L- and N-type calcium channels in the pathophysiology of traumatic spinal cord white matter injury. Neuroscience 99:179-188.

Back SA, Gan X, Li Y, Rosenberg PA, Volpe JJ (1998) Maturation-dependent vulnerability of oligodendrocytes to oxidative stress-induced death caused by glutathione depletion. Journal of Neuroscience 18:6241-6253.

Bal-Price A, Moneer Z, Brown GC (2002) Nitric oxide induces rapid, calcium-dependent release of vesicular glutamate and ATP from cultured rat astrocytes. Glia 40:312-323.

Baraldi PG, Romagnoli R, Tabrizi MA, Falzoni S, di Virgilio F (2000) Synthesis of conformationally constrained analogues of KN62, a potent antagonist of the P2X7-receptor. Bioorg Med Chem Lett 10:681-684.

Baraldi PG, del Carmen Nunez M, Morelli A, Falzoni S, Di Virgilio F, Romagnoli R (2003) Synthesis and biological activity of N-arylpiperazine-modified analogues of KN-62, a potent antagonist of the purinergic P2X7 receptor. J Med Chem 46:1318-1329.

Baraldi PG, Makaeva R, Pavani MG, Nunez Mdel C, Spalluto G, Moro S, Falzoni S, Di Virgilio F, Romagnoli R (2002) Synthesis, biological activity and molecular modeling studies of 1,2,3,4-tetrahydroisoquinoline derivatives as conformationally constrained analogues of KN62, a potent antagonist of the P2X7-receptor containing a tyrosine moiety. Arzneim-Forsch 52:273-285.

Behl C, Davis JB, Lesley R, Schubert D (1994) Hydrogen peroxide mediates amyloid beta protein toxicity. Cell 77:817-827.

Block F, Schwarz M (1996) Memantine reduces functional and morphological consequences induced by global ischemia in rats. Neuroscience letters 208:41-44.

Bolanos JP, Almeida A, Stewart V, Peuchen S, Land JM, Clark JB, Heales SJ (1997) Nitric oxide-mediated mitochondrial damage in the brain: mechanisms and implications for neurodegenerative diseases. J Neurochem 68:2227-2240.

Braughler JM, Hall ED (1992) Involvement of lipid peroxidation in CNS injury. J Neurotrauma 9 Suppl 1:S1-7.

Butt AM, Duncan A, Hornby MF, Kirvell SL, Hunter A, Levine JM, Berry M (1999) Cells expressing the NG2 antigen contact nodes of Ranvier in adult CNS white matter. Glia 26:84-91.

Camello-Almaraz MC, Pozo MJ, Murphy MP, Camello PJ (2006) Mitochondrial production of oxidants is necessary for physiological calcium oscillations. J Cell Physiol 206:487-494.

Chaplin NL, Nieves-Cintron M, Fresquez AM, Navedo MF, Amberg GC (2015) Arterial Smooth Muscle Mitochondria Amplify Hydrogen Peroxide Microdomains Functionally Coupled to L-Type Calcium Channels. Circ Res.

Cornelius C, Crupi R, Calabrese V, Graziano A, Milone P, Pennisi G, Radak Z, Calabrese EJ, Cuzzocrea S (2013) Traumatic brain injury: oxidative stress and neuroprotection. Antioxid Redox Signal 19:836-853.

Dimou L, Gallo V (2015) NG2-glia and their functions in the central nervous system. Glia 63:1429-1451.

Doble A (1999) The role of excitotoxicity in neurodegenerative disease: implications for therapy. Pharmacology & therapeutics 81:163-221.

Duan S, Anderson CM, Keung EC, Chen Y, Chen Y, Swanson RA (2003) P2X7 receptor-mediated release of excitatory amino acids from astrocytes. The Journal of neuroscience : the official journal of the Society for Neuroscience 23:1320-1328.

Dykens JA (1994) Isolated cerebral and cerebellar mitochondria produce free radicals when exposed to elevated CA2+ and Na+: implications for neurodegeneration. Journal of neurochemistry 63:584-591.

Ehrlich M, Knolle E, Ciovica R, Bock P, Turkof E, Grabenwoger M, Cartes-Zumelzu F, Kocher A, Pockberger H, Fang WC, Wolner E, Havel M (1999) Memantine for prevention of spinal cord injury in a rabbit model. The Journal of thoracic and cardiovascular surgery 117:285-291.

Fawcett JW, Asher RA (1999) The glial scar and central nervous system repair. Brain Res Bull 49:377-391.

Fehlings MG, Tator CH, Linden RD (1989) The effect of nimodipine and dextran on axonal function and blood flow following experimental spinal cord injury. J Neurosurg 71:403-416.

Fitzgerald M, Bartlett CA, Harvey AR, Dunlop SA (2010a) Early events of secondary degeneration after partial optic nerve transection: an immunohistochemical study. J Neurotrauma 27:439-452.

Fitzgerald M, Bartlett CA, Harvey AR, Dunlop SA (2010b) Early events of secondary degeneration after partial optic nerve transection: an immunohistochemical study. J Neurotrauma 27:439-452.

Fitzgerald M, Payne SC, Bartlett CA, Evill L, Harvey AR, Dunlop SA (2009) Secondary retinal ganglion cell death and the neuroprotective effects of the calcium channel blocker lomerizine. Invest Ophthalmol Vis Sci 50:5456-5462.

Follett PL, Rosenberg PA, Volpe JJ, Jensen FE (2000) NBQX attenuates excitotoxic injury in developing white matter. Journal of Neuroscience 20:9235-9241.

Gandhi S, Wood-Kaczmar A, Yao Z, Plun-Favreau H, Deas E, Klupsch K, Downward J, Latchman DS, Tabrizi SJ, Wood NW, Duchen MR, Abramov AY (2009) PINK1-associated Parkinson's disease is caused by neuronal vulnerability to calcium-induced cell death. Molecular cell 33:627-638.

Gill R (1994) The pharmacology of alpha-amino-3-hydroxy-5-methyl-4-isoxazole propionate (AMPA)/kainate antagonists and their role in cerebral ischaemia. Cerebrovascular and brain metabolism reviews 6:225-256.

Gomez TM, Spitzer NC (2000) Regulation of growth cone behavior by calcium: new dynamics to earlier perspectives. J Neurobiol 44:174-183.

Graham SH, Chen J, Lan JQ, Simon RP (1996) A dose-response study of neuroprotection using the AMPA antagonist NBQX in rat focal cerebral ischemia. J Pharmacol Exp Ther 276:1-4.

Grynkiewicz G, Poenie M, Tsien RY (1985) A new generation of Ca2+ indicators with greatly improved fluorescence properties. J Biol Chem 260:3440-3450.

Hamilton N, Vayro S, Wigley R, Butt AM (2010) Axons and astrocytes release ATP and glutamate to evoke calcium signals in NG2-glia. Glia 58:66-79.

Hara H, Shimazawa M, Sasaoka M, Yamada C, Iwakura Y, Sakai T, Maeda Y, Yamaguchi T, Sukamoto T, Hashimoto M (1999) Selective effects of lomerizine, a novel diphenylmethylpiperazine Ca2+ channel blocker, on cerebral blood flow in rats and dogs. Clinical and experimental pharmacology & physiology 26:870-876.

Haskew-Layton RE, Payappilly JB, Smirnova NA, Ma TC, Chan KK, Murphy TH, Guo H, Langley B, Sultana R, Butterfield DA, Santagata S, Alldred MJ, Gazaryan IG, Bell GW, Ginsberg SD, Ratan RR (2010) Controlled enzymatic production of astrocytic hydrogen peroxide protects neurons from oxidative stress via an Nrf2-independent pathway. Proc Natl Acad Sci U S A 107:17385-17390.

Hausmann ON (2003) Post-traumatic inflammation following spinal cord injury. Spinal cord 41:369-378.

Herson PS, Lee K, Pinnock RD, Hughes J, Ashford ML (1999) Hydrogen peroxide induces intracellular calcium overload by activation of a non-selective cation channel in an insulin-secreting cell line. The Journal of biological chemistry 274:833-841.

Hollmann M, Hartley M, Heinemann S (1991) Ca2+ permeability of KA-AMPA--gated glutamate receptor channels depends on subunit composition. Science 252:851-853.

Huang CY, Wang LC, Wang HK, Pan CH, Cheng YY, Shan YS, Chio CC, Tsai KJ (2015) Memantine alleviates brain injury and neurobehavioral deficits after experimental subarachnoid hemorrhage. Mol Neurobiol 51:1038-1052.

Huang X, Li Q, Li H, Guo L (2009) Neuroprotective and antioxidative effect of cactus polysaccharides in vivo and in vitro. Cell Mol Neurobiol 29:1211-1221.

Kahlert S, Zundorf G, Reiser G (2005) Glutamate-mediated influx of extracellular Ca2+ is coupled with reactive oxygen species generation in cultured hippocampal neurons but not in astrocytes. Journal of neuroscience research 79:262-271.

Kaneko M, Beamish RE, Dhalla NS (1989) Depression of heart sarcolemmal Ca2+-pump activity by oxygen free radicals. Am J Physiol Heart Circ Physiol 256:H368-H374.

Katsetos CD, Frankfurter A, Christakos S, Mancall EL, Vlachos IN, Urich H (1993) Differential localization of class III, beta-tubulin isotype and calbindin-D28k defines distinct neuronal types in the developing human cerebellar cortex. Journal of neuropathology and experimental neurology 52:655-666.

Kerschensteiner M, Schwab ME, Lichtman JW, Misgeld T (2005) In vivo imaging of axonal degeneration and regeneration in the injured spinal cord. Nat Med 11:572-577.

Klein KU, Engelhard K (2010) Perioperative neuroprotection. Best practice & research Clinical anaesthesiology 24:535-549.

Komuro H, Rakic P (1996) Intracellular Ca2+ fluctuations modulate the rate of neuronal migration. Neuron 17:275-285.

Kowaltowski AJ, de Souza-Pinto NC, Castilho RF, Vercesi AE (2009a) Mitochondria and reactive oxygen species. Free Radic Biol Med 47:333-343.

Kowaltowski AJ, de Souza-Pinto NC, Castilho RF, Vercesi AE (2009b) Mitochondria and reactive oxygen species. Free Radic Biol Med 47:333-343.

Kristian T, Siesjo BK (1998) Calcium in ischemic cell death. Stroke 29:705-718.

Lau A, Tymianski M (2010) Glutamate receptors, neurotoxicity and neurodegeneration. European journal of physiology 460:525-542.

Lipton P (1999) Ischemic cell death in brain neurons. Physiol Rev 79:1431-1568.

Liu XZ, Xu XM, Hu R, Du C, Zhang SX, McDonald JW, Dong HX, Wu YJ, Fan GS, Jacquin MF, Hsu CY, Choi DW (1997) Neuronal and glial apoptosis after traumatic spinal cord injury. Journal of Neuroscience 17:5395-5406.

Ma S, Liu H, Jiao H, Wang L, Chen L, Liang J, Zhao M, Zhang X (2012) Neuroprotective effect of ginkgolide K on glutamate-induced cytotoxicity in PC 12 cells via inhibition of ROS generation and Ca(2+) influx. Neurotoxicology 33:59-69.

Mandavilli BS, Boldogh I, Van Houten B (2005) 3-nitropropionic acid-induced hydrogen peroxide, mitochondrial DNA damage, and cell death are attenuated by Bcl-2 overexpression in PC12 cells. Brain research Molecular brain research 133:215-223.

Matute C (2006) Oligodendrocyte NMDA receptors: a novel therapeutic target. Trends Mol Med 12:289-292.

Matute C, Domercq M, Sanchez-Gomez MV (2006) Glutamate-mediated glial injury: mechanisms and clinical importance. Glia 53:212-224.

Matute C, Sanchez-Gomez MV, Martinez-Millan L, Miledi R (1997) Glutamate receptor-mediated toxicity in optic nerve oligodendrocytes. Proc Natl Acad Sci U S A 94:8830-8835.

Matute C, Torre I, Perez-Cerda F, Perez-Samartin A, Alberdi E, Etxebarria E, Arranz AM, Ravid R, Rodriguez-Antiguedad A, Sanchez-Gomez M, Domercq M (2007) P2X(7) receptor blockade prevents ATP excitotoxicity in oligodendrocytes and ameliorates experimental autoimmune encephalomyelitis. Journal of Neuroscience 27:9525-9533.

McAllister J, Ghosh S, Berry D, Park M, Sadeghi S, Wang KX, Parker WD, Swerdlow RH (2008) Effects of memantine on mitochondrial function. Biochemical pharmacology 75:956-964.

Muralidharan P, Cserne Szappanos H, Ingley E, Hool L (2016) Evidence for redox sensing by a human cardiac calcium channel. Sci Rep 6:19067.

Neary JT, Kang Y, Tran M, Feld J (2005) Traumatic injury activates protein kinase B/Akt in cultured astrocytes: role of extracellular ATP and P2 purinergic receptors. J Neurotrauma 22:491-500.

Nicotera P, Rossi A (1994) Nuclear Ca2+: physiological regulation and role in apoptosis. Mol Cell Biochem 135:89-98.

Nishida K, Nakatani T, Ohishi A, Okuda H, Higashi Y, Matsuo T, Fujimoto S, Nagasawa K (2012) Mitochondrial dysfunction is involved in P2X7 receptor-mediated neuronal cell death. Journal of neurochemistry 122:1118-1128.

O'Hare Doig RL, Bartlett CA, Maghzal GJ, Lam M, Archer M, Stocker R, Fitzgerald M (2014a) Reactive species and oxidative stress in optic nerve vulnerable to secondary degeneration. Exp Neurol 261C:136-146.

O'Hare Doig RL, Bartlett CA, Maghzal GJ, Lam M, Archer M, Stocker R, Fitzgerald M (2014b) Reactive species and oxidative stress in optic nerve vulnerable to secondary degeneration. Exp Neurol 261:136-146.

Ouardouz M, Nikolaeva MA, Coderre E, Zamponi GW, McRory JE, Trapp BD, Yin X, Wang W, Woulfe J, Stys PK (2003) Depolarization-induced Ca2+ release in ischemic spinal cord white matter involves L-type Ca2+ channel activation of ryanodine receptors. Neuron 40:53-63.

Payne SC, Bartlett CA, Harvey AR, Dunlop SA, Fitzgerald M (2011) Chronic swelling and abnormal myelination during secondary degeneration after partial injury to a central nervous system tract. J Neurotrauma 28:1077-1088.

Prilloff S, Noblejas MI, Chedhomme V, Sabel BA (2007) Two faces of calcium activation after optic nerve trauma: life or death of retinal ganglion cells in vivo depends on calcium dynamics. Eur J Neurosci 25:3339-3346.

Richardson WD, Young KM, Tripathi RB, McKenzie I (2011) NG2-glia as multipotent neural stem cells: fact or fantasy? Neuron 70:661-673.

Rojanasakul Y, Wang L, Hoffman AH, Shi X, Dalal NS, Banks DE, Ma JKH (1993) Mechanisms of Hydroxyl Free Radical-induced Cellular Injury and Calcium Overloading in Alveolar Macrophages. Am J Respir Cell Mol Biol 8:377-383.

Roveri A, Coassin M, Maiorino M, Zamburlini A, van Amsterdam FTM, Ratti E, Ursini F (1992) Effect of hydrogen peroxide on calcium homeostasis in smooth muscle cells. Arch Biochem Biophys 297:265-270.

Savigni DL, O'Hare Doig RL, Szymanski CR, Bartlett CA, Lozic I, Smith NM, Fitzgerald M (2013) Three Ca2+ channel inhibitors in combination limit chronic secondary degeneration following neurotrauma. Neuropharmacology 75:380-390.

Spitzer NC, Lautermilch NJ, Smith RD, Gomez TM (2000) Coding of neuronal differentiation by calcium transients. BioEssays 22:811-817.

Stack EC, Smith KM, Ryu H, Cormier K, Chen M, Hagerty SW, Del Signore SJ, Cudkowicz ME, Friedlander RM, Ferrante RJ (2006) Combination therapy using minocycline and coenzyme Q10 in R6/2 transgenic Huntington's disease mice. Biochim Biophys Acta 1762:373-380.

Suadicani SO, Cherkas PS, Zuckerman J, Smith DN, Spray DC, Hanani M (2010) Bidirectional calcium signaling between satellite glial cells and neurons in cultured mouse trigeminal ganglia. Neuron Glia Biol 6:43-51.

Szymanski CR, Chiha W, Morellini N, Cummins N, Bartlett CA, O'Hare Doig RL, Savigni DL, Payne SC, Harvey AR, Dunlop SA, Fitzgerald M (2013) Paranode abnormalities and oxidative stress in optic nerve vulnerable to secondary degeneration: modulation by 670 nm light treatment. PLoS One 8:e66448.

Takadera T, Ohtsuka M, Aoki H (2010) Chelation of extracellular calcium-induced cell death was prevented by glycogen synthase kinase-3 inhibitors in PC12 cells. Cell Mol Neurobiol 30:193-198.

Takahashi M, Ni JW, Kawasaki-Yatsugi S, Toya T, Ichiki C, Yatsugi SI, Koshiya K, Shimizu-Sasamata M, Yamaguchi T (1998) Neuroprotective efficacy of YM872, an alpha-amino-3-hydroxy-5-methylisoxazole-4-propionic acid receptor antagonist, after permanent middle cerebral artery occlusion in rats. J Pharmacol Exp Ther 287:559-566.

Tamaki Y, Araie M, Fukaya Y, Nagahara M, Imamura A, Honda M, Obata R, Tomita K (2003) Effects of lomerizine, a calcium channel antagonist, on retinal and optic nerve head circulation in rabbits and humans. Invest Ophthalmol Vis Sci 44:4864-4871.

Tanaka T, Nangaku M, Miyata T, Inagi R, Ohse T, Ingelfinger JR, Fujita T (2004) Blockade of calcium influx through L-type calcium channels attenuates mitochondrial injury and apoptosis in hypoxic renal tubular cells. J Am Soc Nephrol 15:2320-2333.

Tekkok SB, Goldberg MP (2001) Ampa/kainate receptor activation mediates hypoxic oligodendrocyte death and axonal injury in cerebral white matter. Journal of Neuroscience 21:4237-4248.

Totoiu MO, Keirstead HS (2005) Spinal cord injury is accompanied by chronic progressive demyelination. J Comp Neurol 486:373-383.

Tuszynski MH (2005) New strategies for CNS repair. Ernst Schering Res Found Workshop:1-10.

Tymianski M, Charlton MP, Carlen PL, Tator CH (1993) Source specificity of early calcium neurotoxicity in cultured embryonic spinal neurons. Journal of Neuroscience 13:2085-2104.

van den Pol AN, Finkbeiner SM, Cornell-Bell AH (1992) Calcium excitability and oscillations in suprachiasmatic nucleus neurons and glia in vitro. J Neurosci 12:2648-2664.

Viola HM, Arthur PG, Hool LC (2007) Transient exposure to hydrogen peroxide causes an increase in mitochondria-derived superoxide as a result of sustained alteration in L-type Ca2+ channel function in the absence of apoptosis in ventricular myocytes. Circ Res 100:1036-1044.

Wang X, Arcuino G, Takano T, Lin J, Peng WG, Wan P, Li P, Xu Q, Liu QS, Goldman SA, Nedergaard M (2004) P2X7 receptor inhibition improves recovery after spinal cord injury. Nat Med 10:821-827.

Weishaupt N, Silasi G, Colbourne F, Fouad K (2010) Secondary damage in the spinal cord after motor cortex injury in rats. J Neurotrauma 27:1387-1397.

Whittemore ER, Loo DT, Cotman CW (1994) Exposure to hydrogen peroxide induces cell death via apoptosis in cultured rat cortical neurons. Neuroreport 5:1485-1488.

Xue D, Huang ZG, Barnes K, Lesiuk HJ, Smith KE, Buchan AM (1994) Delayed treatment with AMPA, but not NMDA, antagonists reduces neocortical infarction. Journal of Cerebral Blood Flow and Metabolism 14:251-261.

Ye ZC, Wyeth MS, Baltan-Tekkok S, Ransom BR (2003) Functional hemichannels in astrocytes: a novel mechanism of glutamate release. The Journal of neuroscience : the official journal of the Society for Neuroscience 23:3588-3596.

Zhang Z, He Y, Tuteja D, Xu D, Timofeyev V, Zhang Q, Glatter KA, Xu Y, Shin HS, Low R, Chiamvimonvat N (2005) Functional roles of Cav1.3(alpha1D) calcium channels in atria: insights gained from gene-targeted null mutant mice. Circulation 112:1936-1944.

Highlights

- The effects of combinations of Ca^{2+} channel inhibitors on H_2O_2 stressed cells were assessed *in vitro.*
- Most combinations of inhibitors with oxATP decreased Ca^{2+} influx and increased cell viability.
- However, reductions in intracellular Ca^{2+} concentration were not always linked to cell viability.
- Combinations of inhibitors preserved some cell subpopulations, particularly NG2+/olig2- glia.
- The data increase understanding of the efficacy of Ca^{2+} channel inhibitor combinations *in vivo*

Figure 1

Click here to download high resolution image

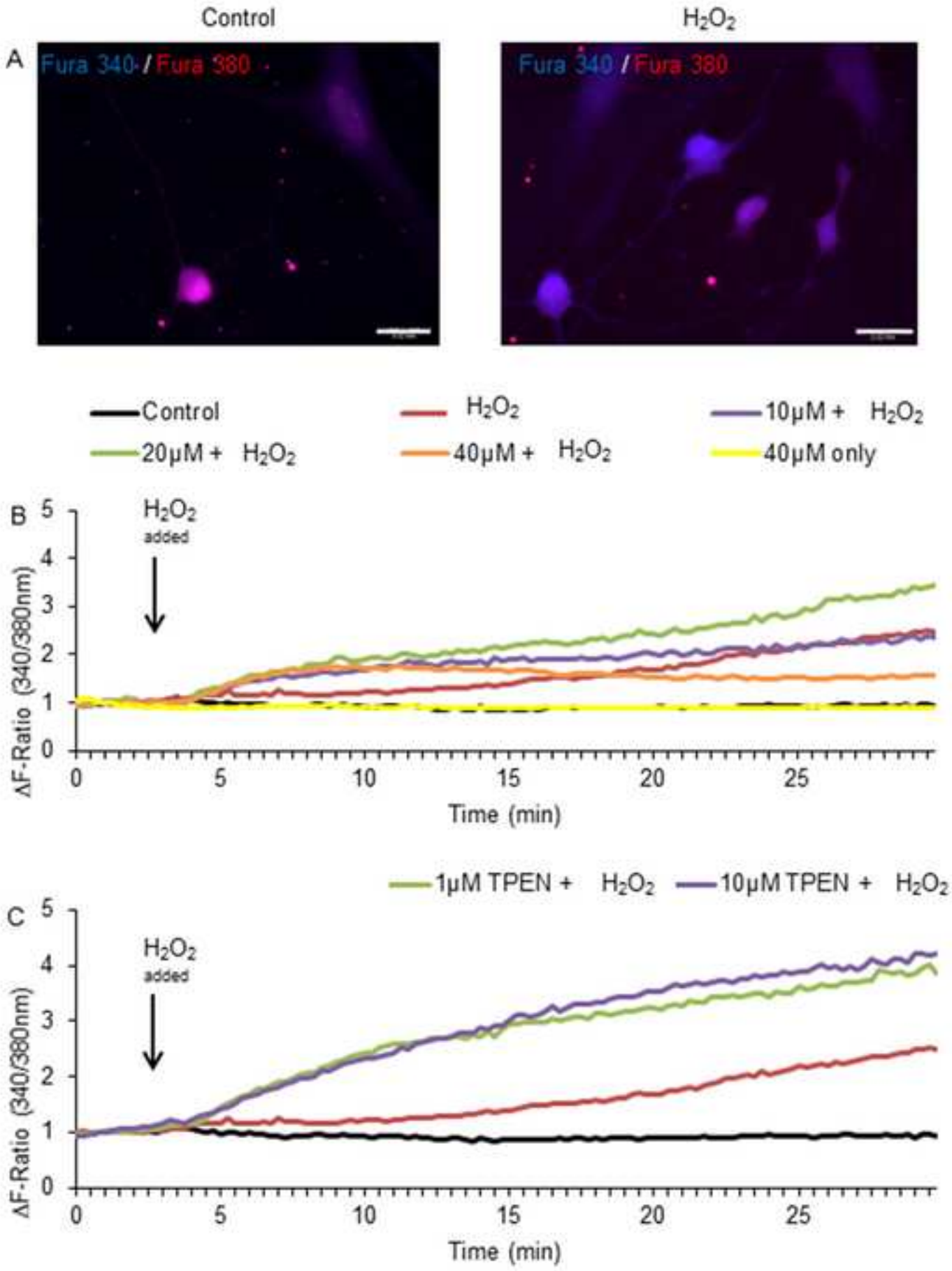

Figure 2

Click here to download high resolution image

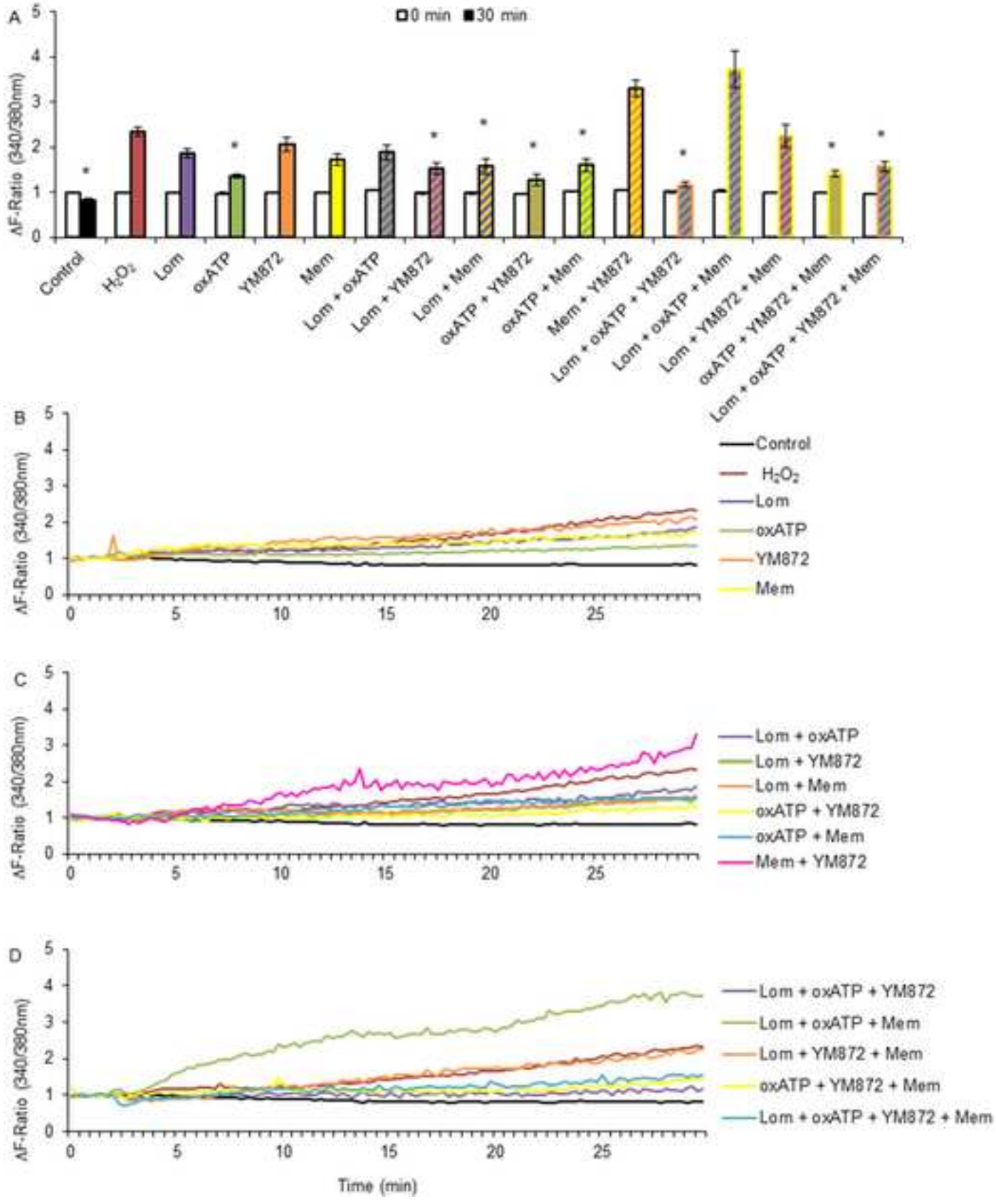

Figure 3

Click here to download high resolution image

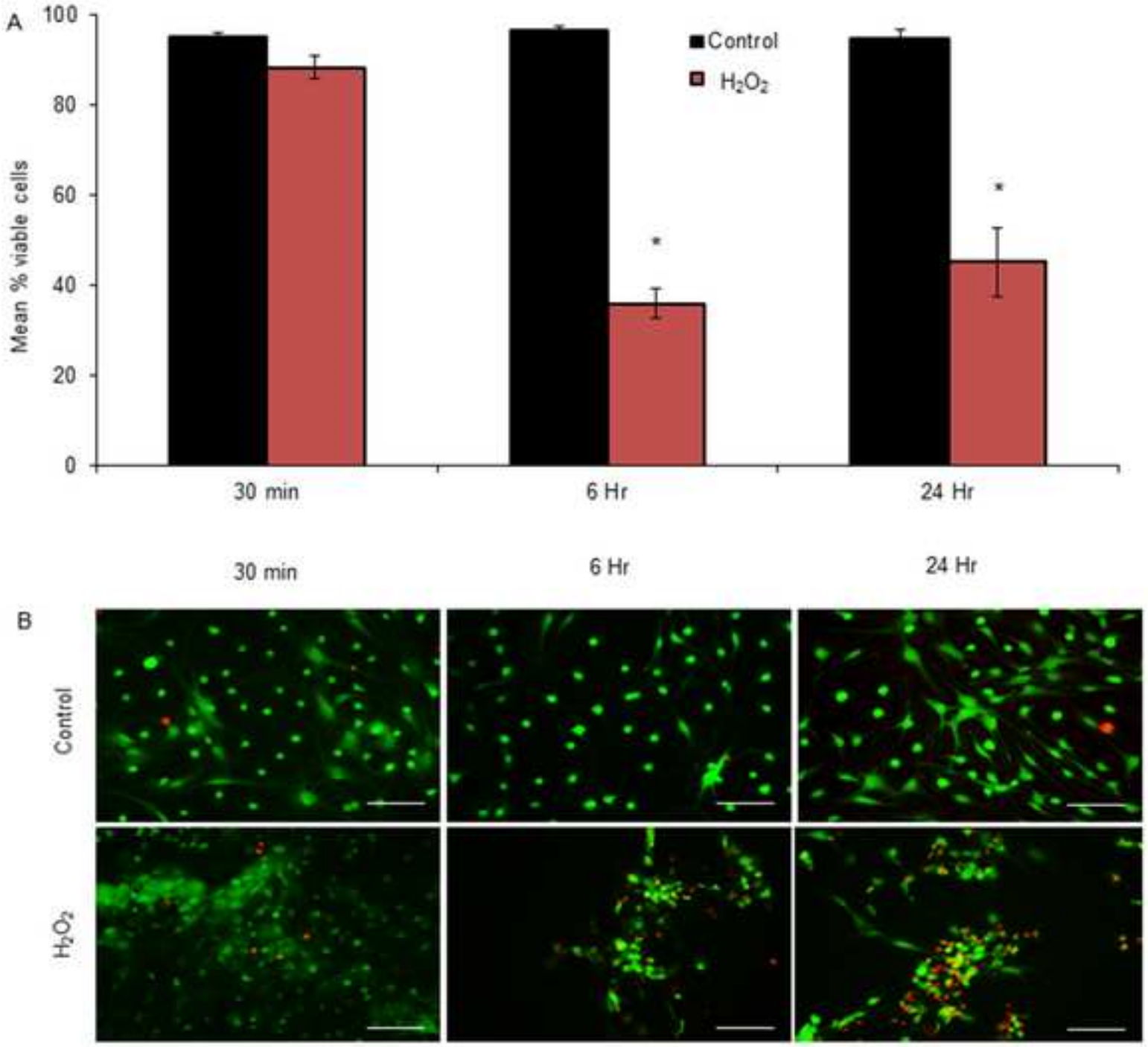

Figure 4

Click here to download high resolution image

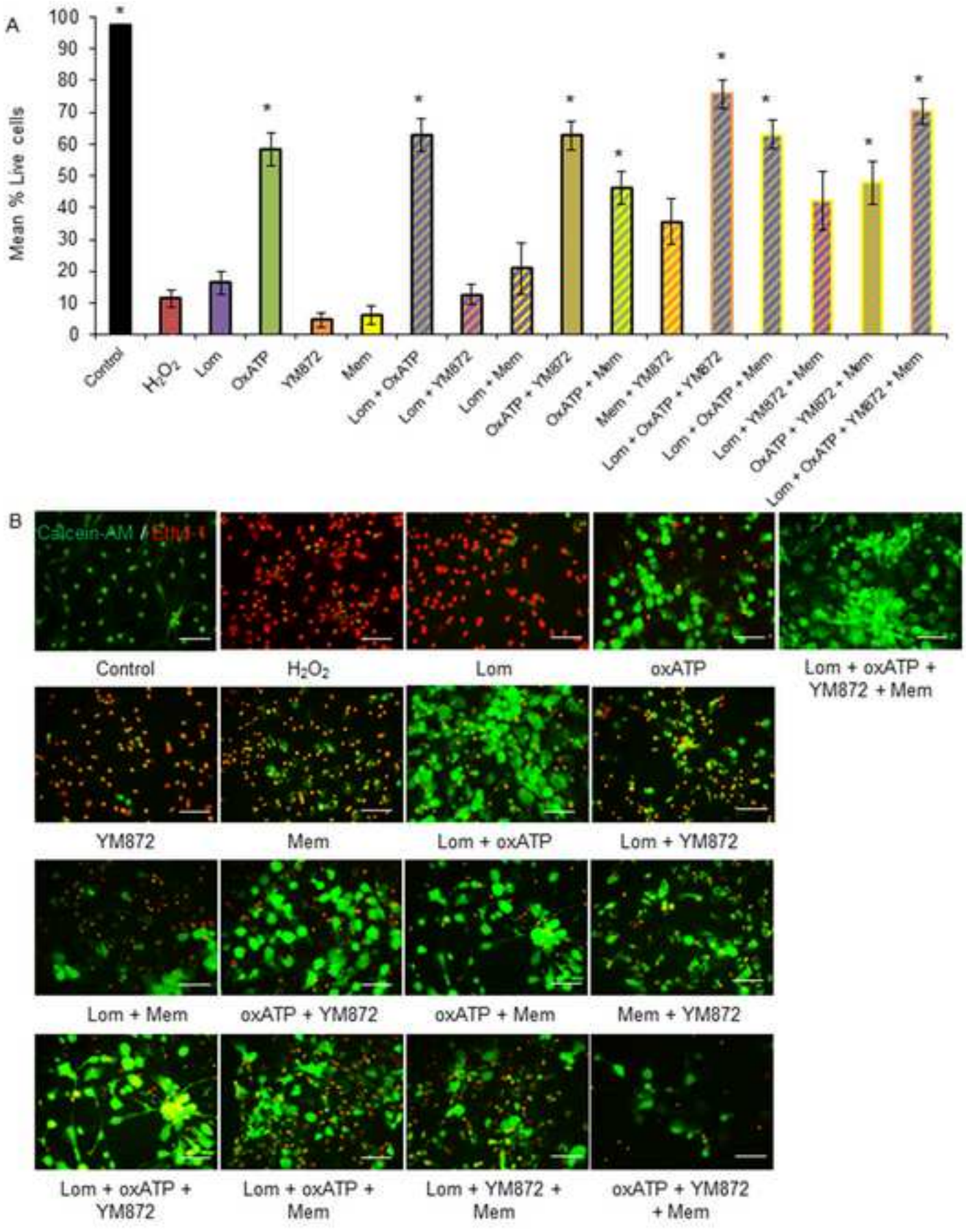

Figure 5

Click here to download high resolution image

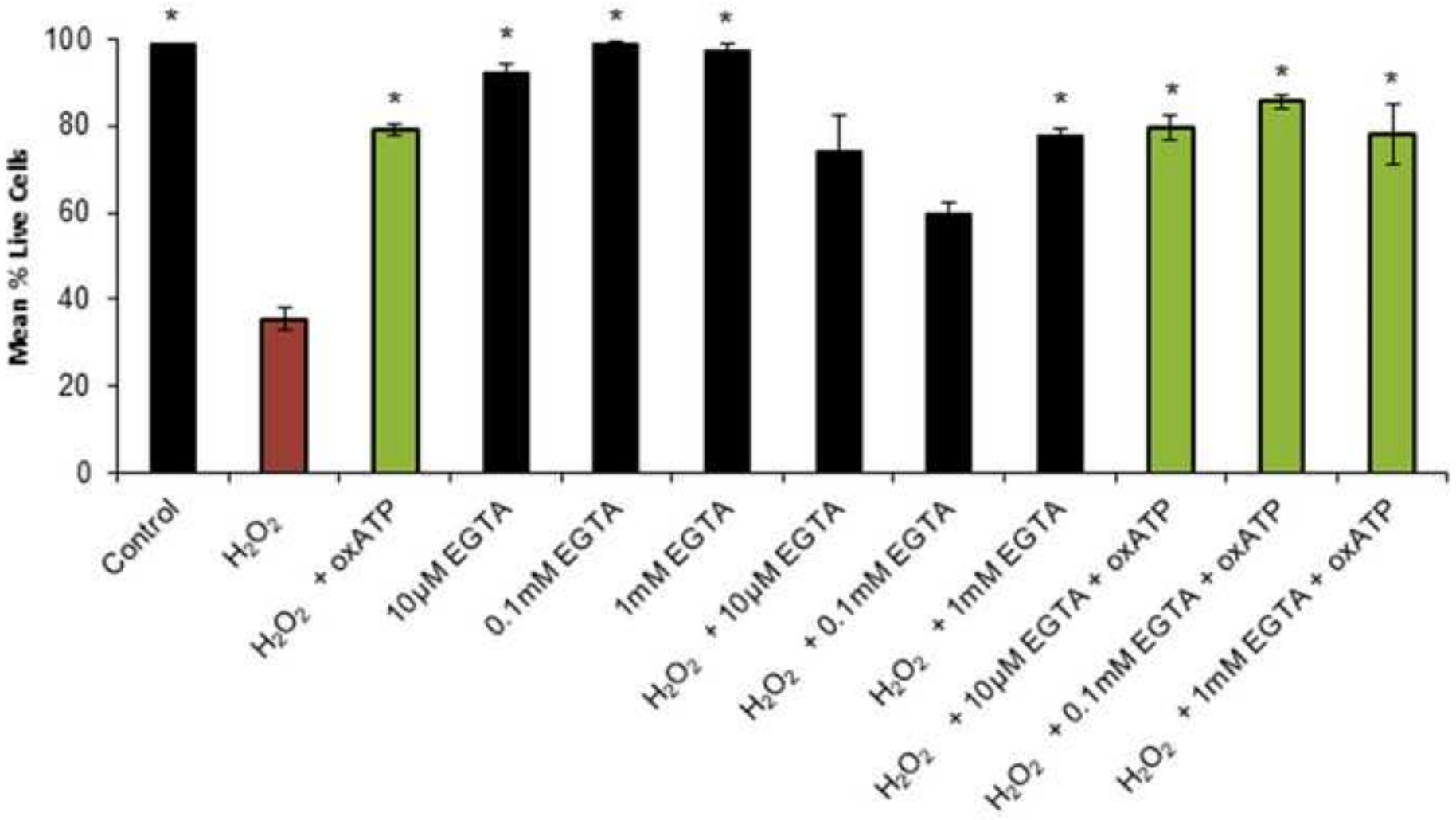

Figure 6

Click here to download high resolution image